

Electronic Supplementary Information

Novel Pyrene-Calix[4]arene Derivatives as Highly Sensitive Sensors for Nucleotides, DNA and RNA

Ivana Nikšić-Franjić,^a Benoit Collason,^b Olivia Reinaud,^b Aleksandar Višnjevac,^{a,*} Ivo Piantanida^c and Dijana Pavlović Saftić^{c,*}

^a *Division of Physical Chemistry, Laboratory for chemical and biological crystallography, Ruđer Bošković Institute, Bijenička cesta 54, 10000 Zagreb, Croatia*

^b *Université de Paris - Laboratoire de Chimie et Biochimie Pharmacologiques et Toxicologiques, CNRS UMR 8601, 45 rue des Saints Pères, 75006 Paris, France*

^c *Division of Organic Chemistry and Biochemistry, Laboratory for Biomolecular Interactions and Spectroscopy, Ruđer Bošković Institute, Bijenička cesta 54, 10000 Zagreb, Croatia*

*Corresponding authors:

Dijana Pavlović-Saftić, e-mail: dijana.pavlovic.saftic@irb.hr

Aleksandar Višnjevac, e-mail: aleksandar.visnjevac@irb.hr

Contents

1. NMR and HRMS spectra of 2 and 3	1
3. Interactions with DNA and RNA	11
3.1. Spectrophotometric titrations with mono- and polynucleotides	12
3.2. Circular dichroism (CD) experiments	30
3.3. Thermal denaturation experiments	34

1. NMR and HRMS spectra of 2 and 3

General procedures

Solvents were distilled from appropriate drying agents shortly before use. TLC was carried out on DC-plastikfolien Kieselgel 60 F₂₅₄ and preparative thick layer (2 mm) chromatography was done on Merck 60 F₂₅₄. ¹H and ¹³C NMR spectra were recorded in CD₃CN on Bruker AV 600 MHz spectrometers. Chemical shifts (δ) are expressed in ppm, and *J* values in Hz. Signal multiplicities are denoted as s (singlet), d (doublet), t (triplet), q (quartet) and m (multiplet). High resolution mass spectra (HRMS) were obtained using a MALDI-TOF/TOF mass spectrometer 4800 Plus MALDI TOF/TOF analyzer (Applied Biosystems Inc., Foster City, CA, USA).

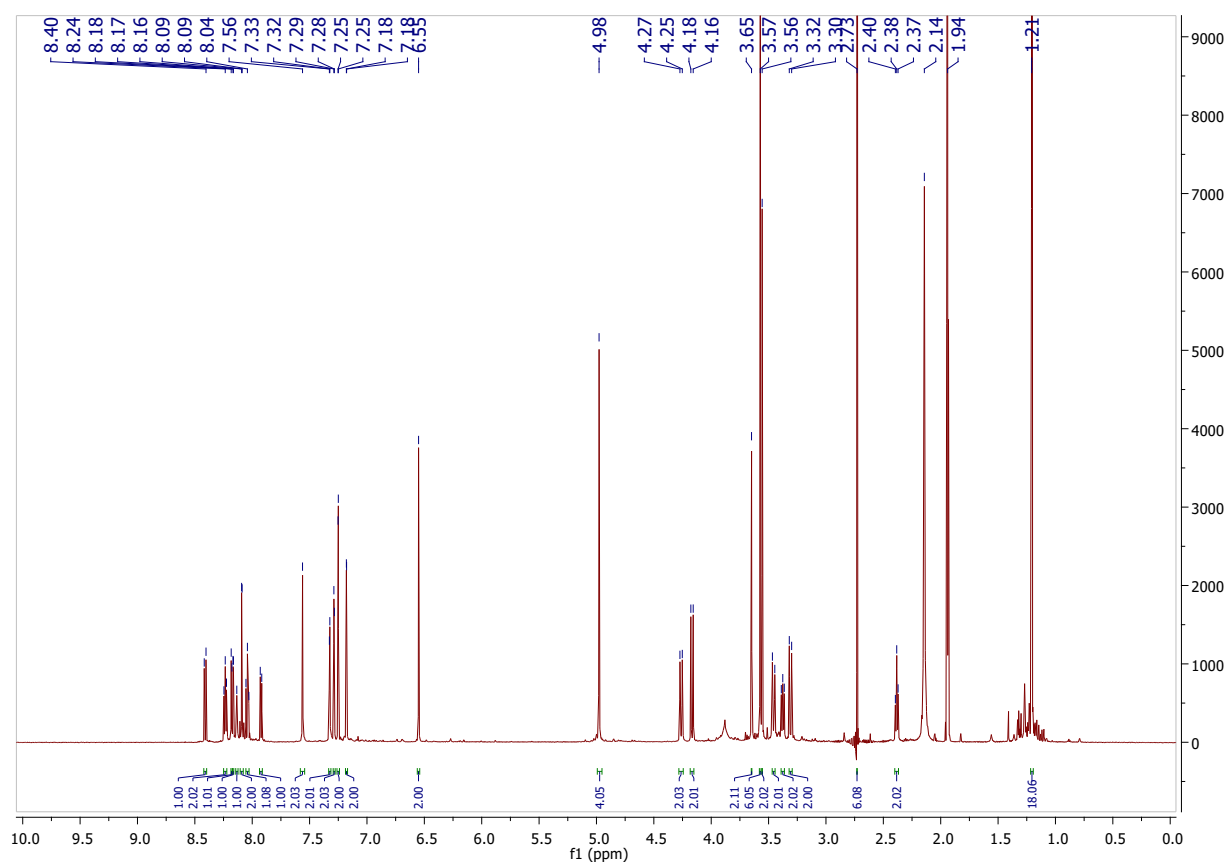


Figure S1. ¹H NMR (600 MHz) spectrum of compound 2 recorded in CD₃CN.

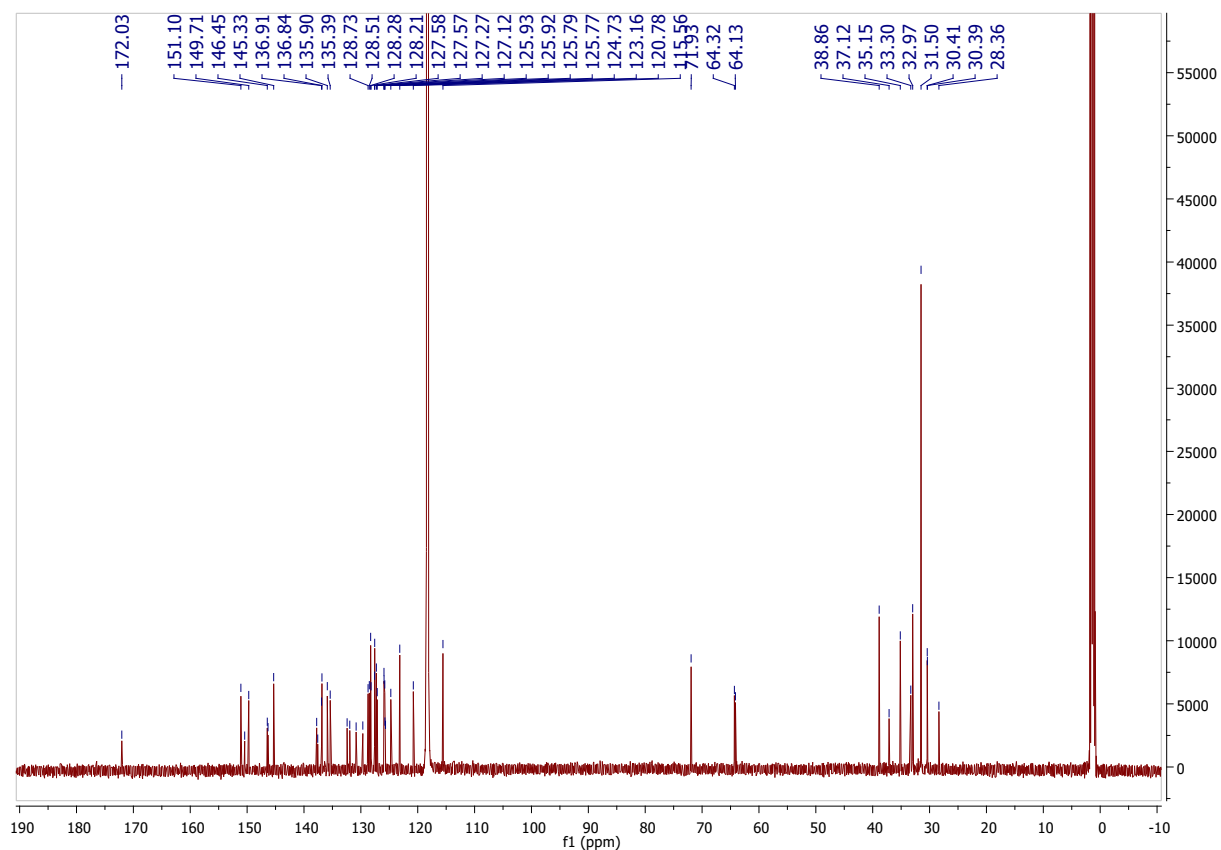


Figure S2. ^{13}C NMR (151 MHz) spectrum of compound **2** recorded in CD_3CN .

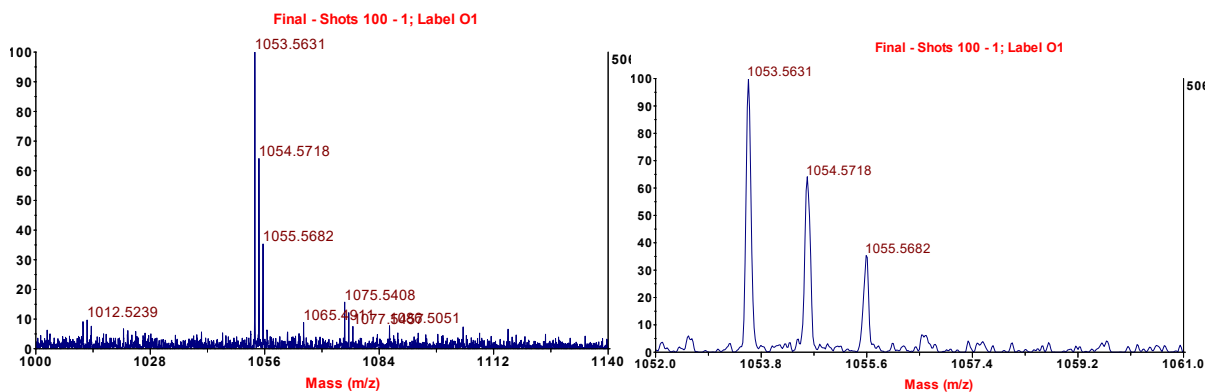


Figure S3. MALDI TOF/TOF mass spectrum of compound **2** in the range m/z 1000 – 1140 (left), and magnification of the spectrum from m/z 1052 to m/z 1061 (right).

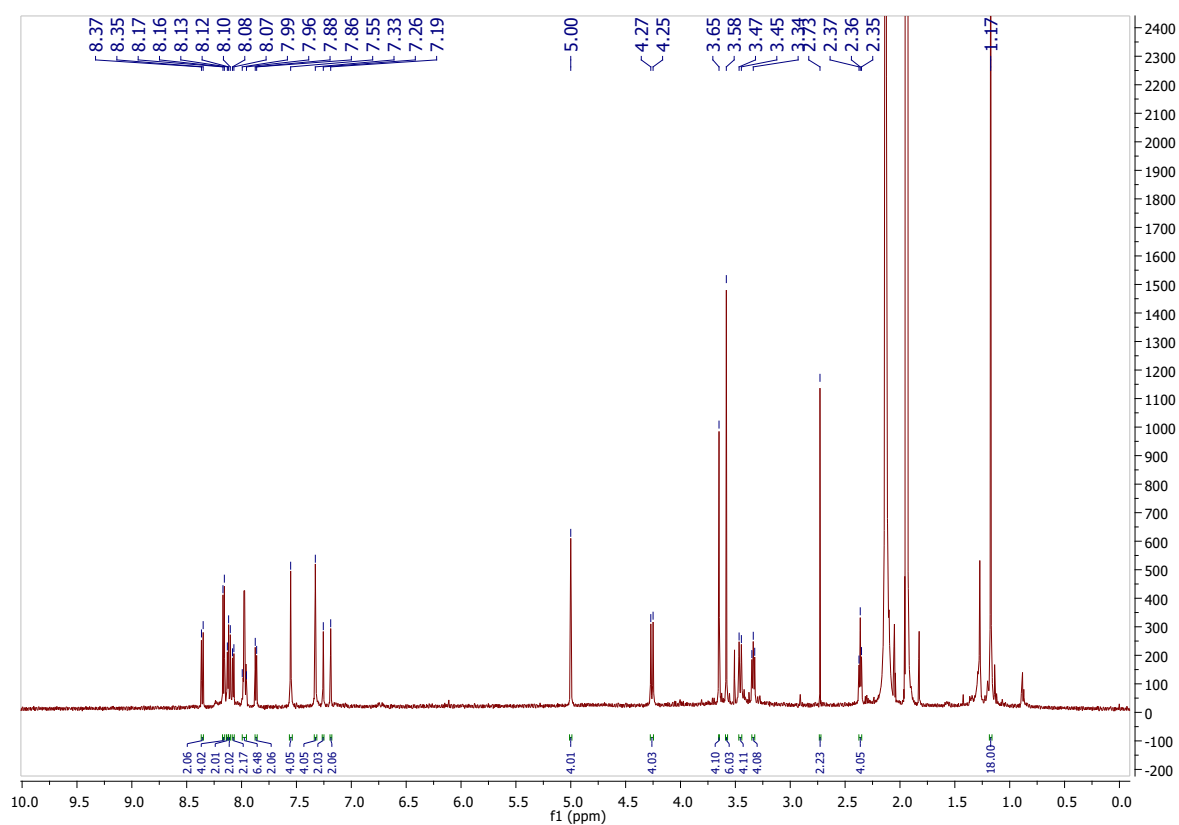


Figure S4. ^1H NMR (600 MHz) spectrum of compound **3** recorded in CD_3CN .

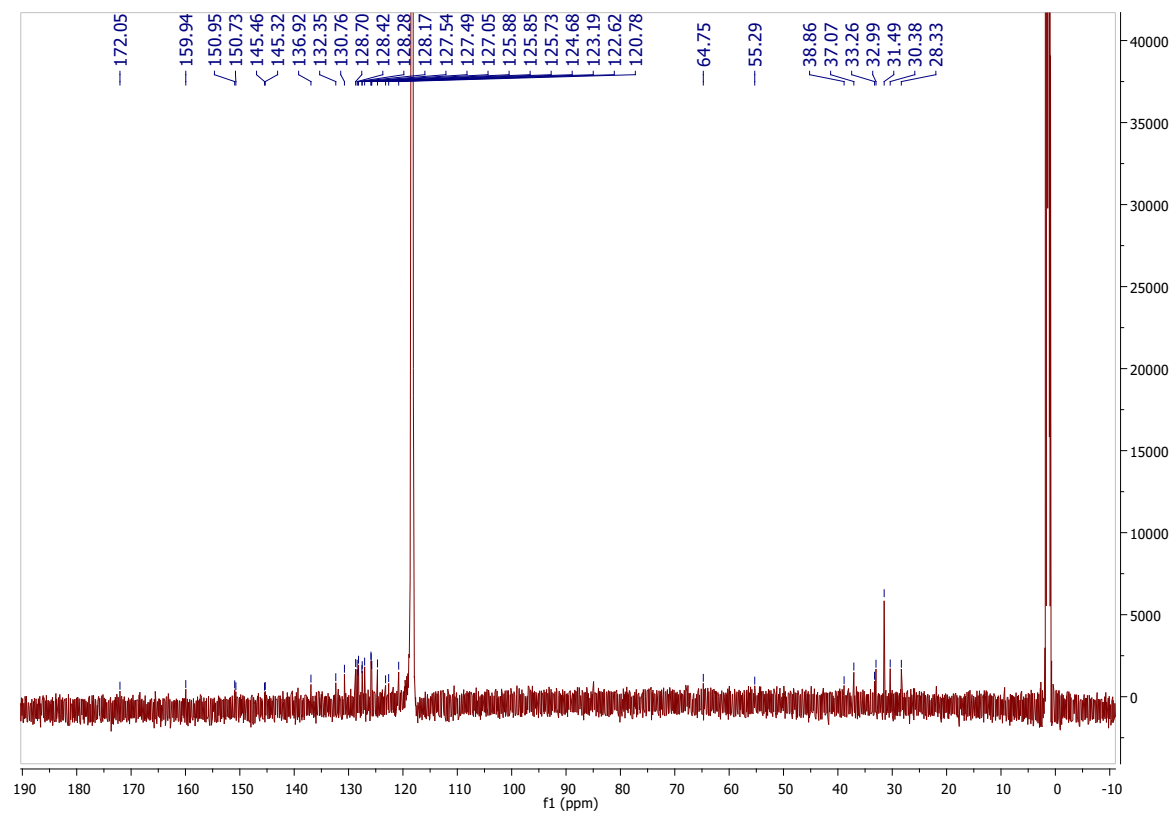


Figure S5. ^{13}C NMR (151 MHz) spectrum of compound **3** recorded in CD_3CN .

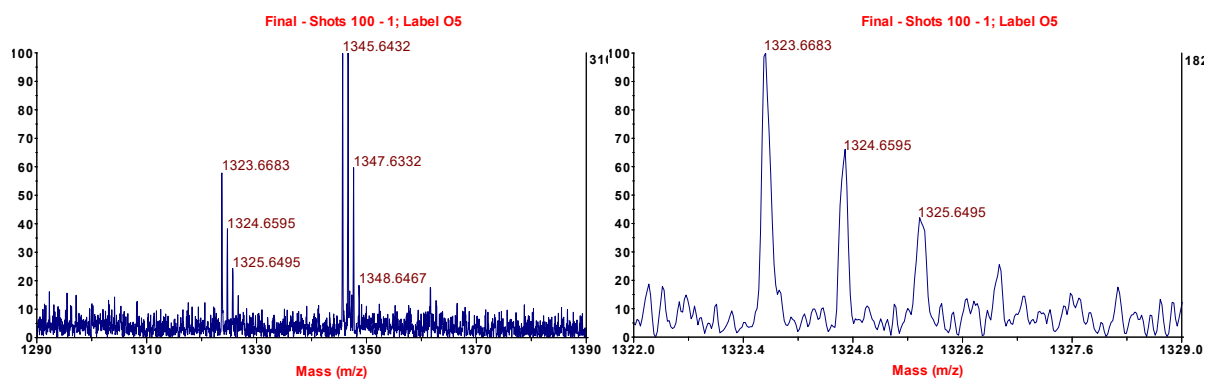


Figure S6. MALDI TOF/TOF mass spectrum of compound **3** in the range m/z 1290 – 1390 (left), and magnification of the spectrum from m/z 1322 to m/z 1329 (right).

2. Spectrofluorimetric and photophysical characterization

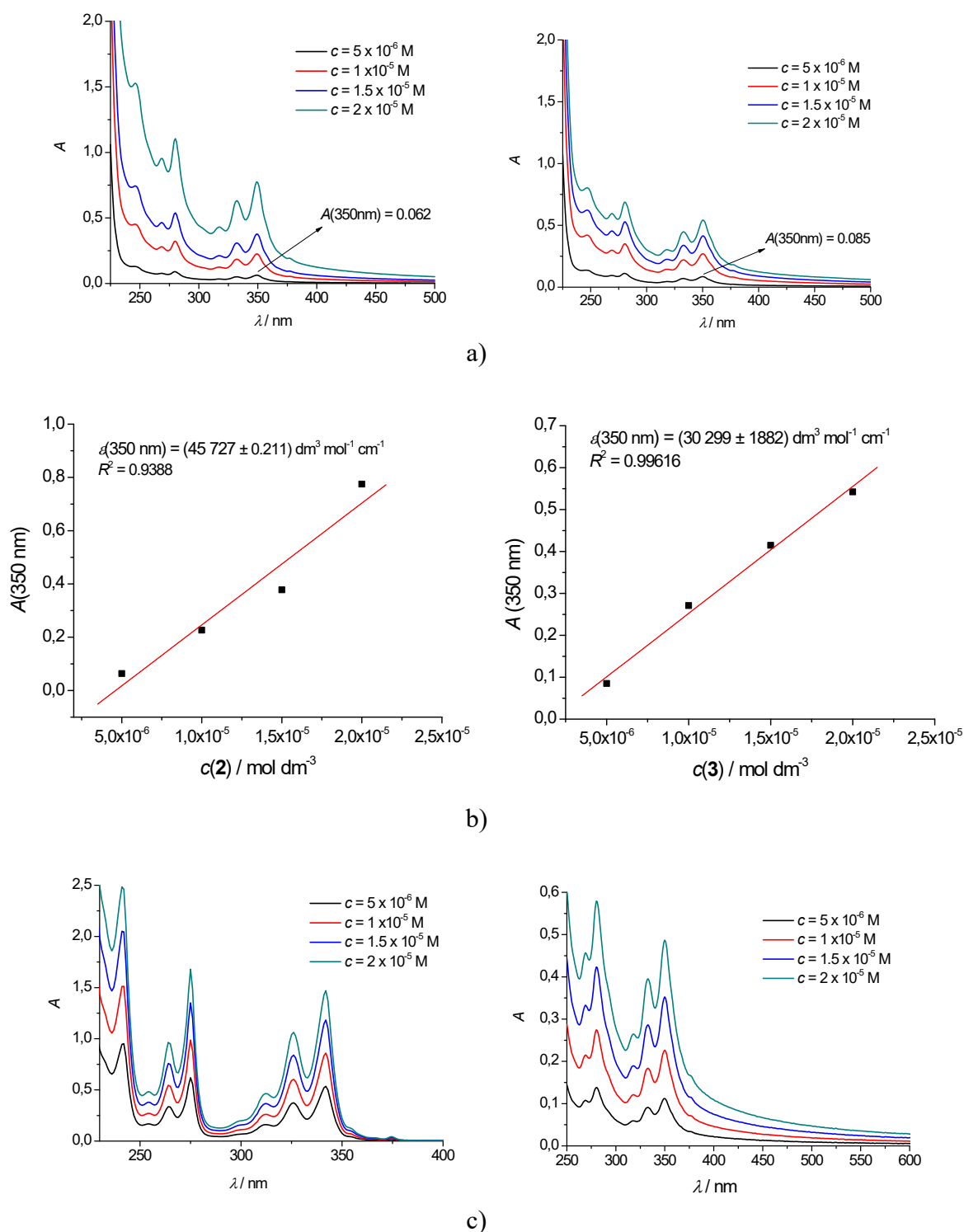


Figure S7. (a) UV/Vis spectra of studied conjugates **2** and **3** in water (0.1% DMSO); (b) absorbance dependence on $c(2)$ or $c(3)$ ($c = 5 \times 10^{-6} - 2 \times 10^{-5} \text{ M}$); (c) UV/Vis spectra of referent compounds 1-pyrenebutyric acid (**A**) and **B** in buffered solution pH 7, $I = 0.05 \text{ M}$.

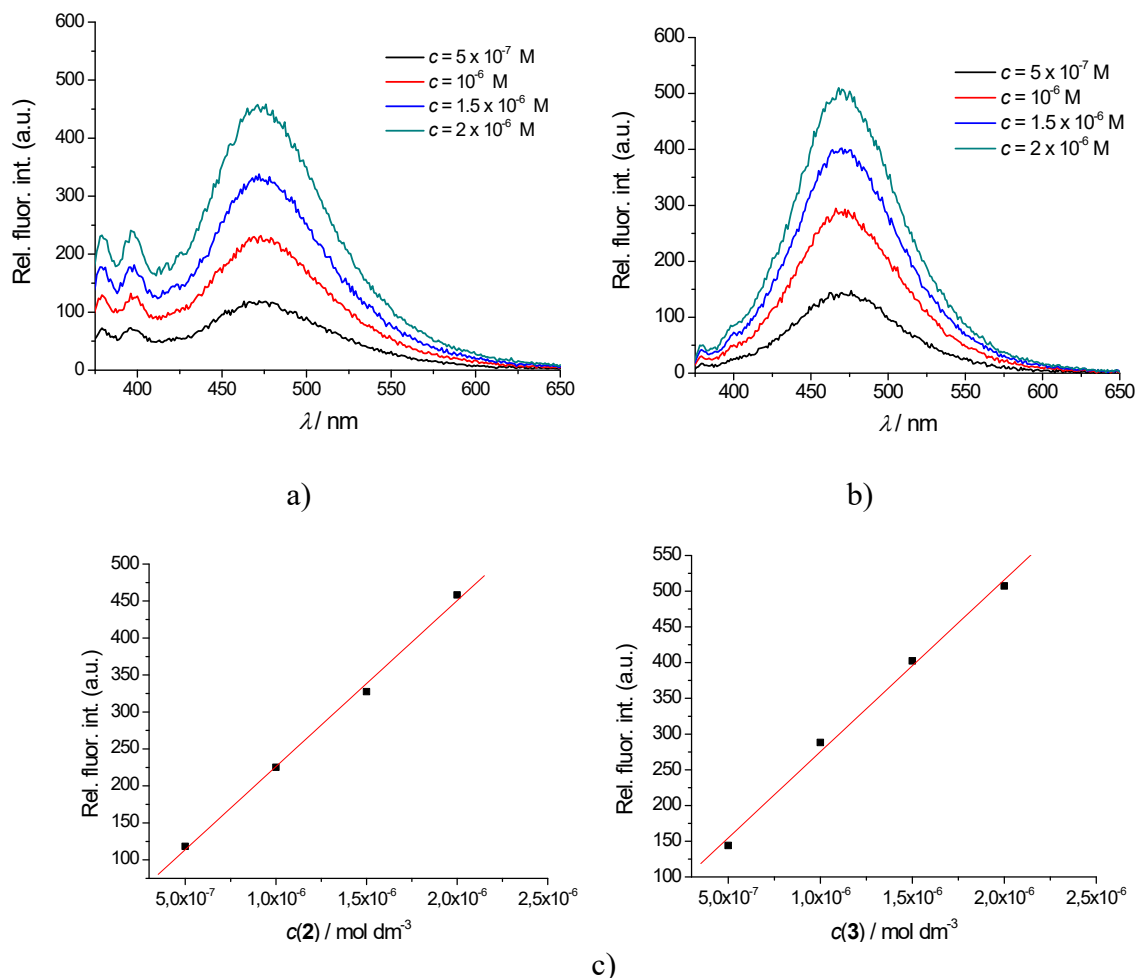


Figure S8. Fluorescence spectra of: a) **2** and b) **3**; c) relative fluorescence dependence on $c(2)$ or $c(3)$ ($c = 5 \times 10^{-7} - 2 \times 10^{-6}$ M) at $\lambda_{\text{em}} = 475$ nm. Done in water, $\lambda_{\text{exc}} = 350$ nm.

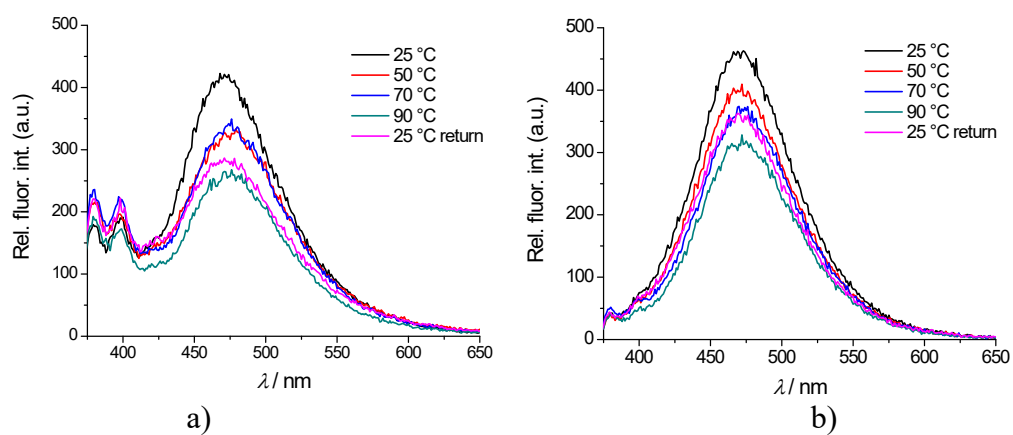


Figure S9. Temperature dependence of: a) **2** and b) **3** at concentration $c = 2 \times 10^{-6}$ M. Done in water, $\lambda_{\text{exc}} = 350$ nm.

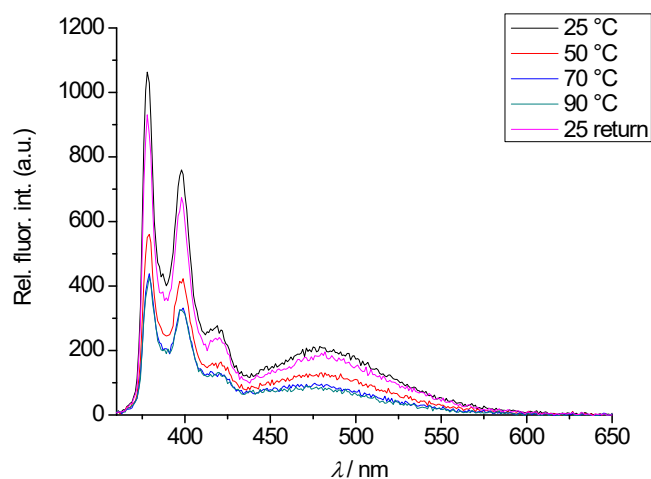


Figure S10. Temperature dependence of **3** at concentration $c = 2 \times 10^{-6}$ M. Done in DMSO, $l = 1$ cm, $\lambda_{\text{exc}} = 350$ nm.

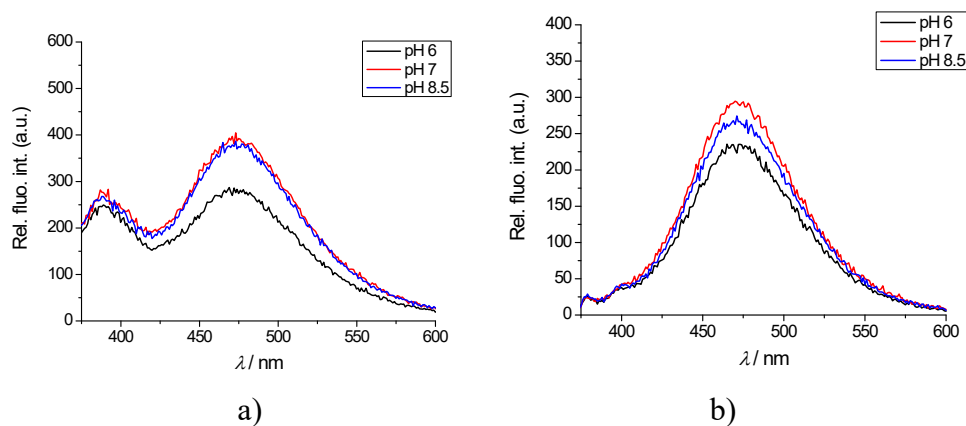
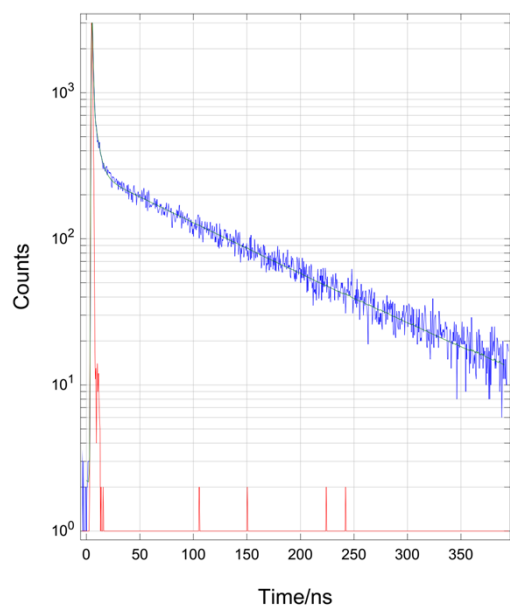
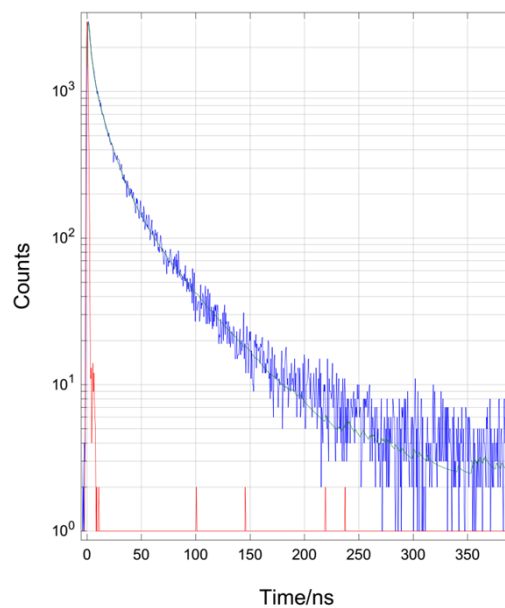


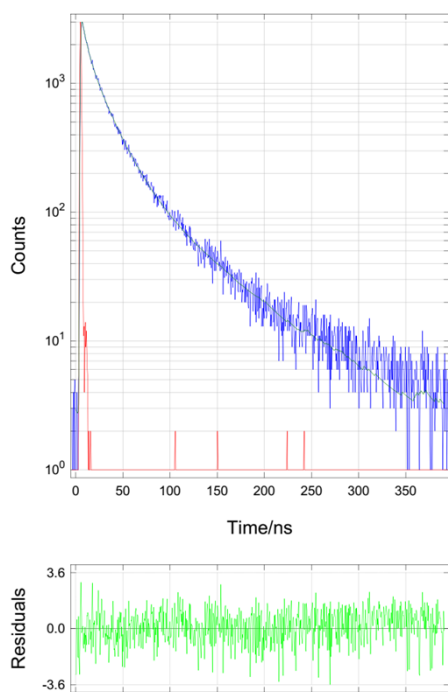
Figure S11. The dependence of the fluorescence spectra of compounds **2** (a) and **3** (b) ($c = 1 \times 10^{-6}$ M) on pH. Done in phosphate buffer adjusted to various pH values by buffer preparation protocol.



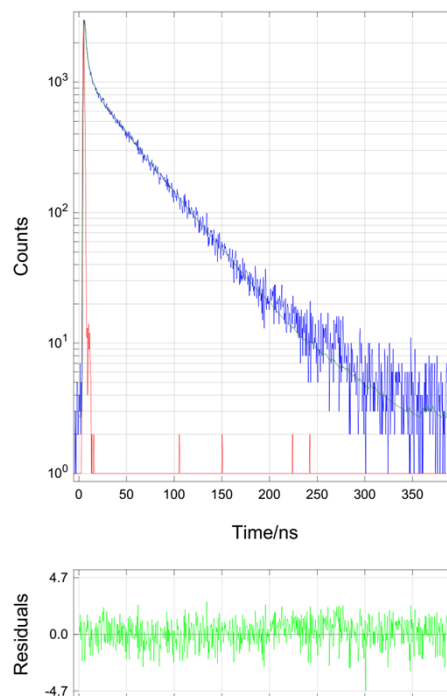
a) 400 nm, water



b) 475 nm, water

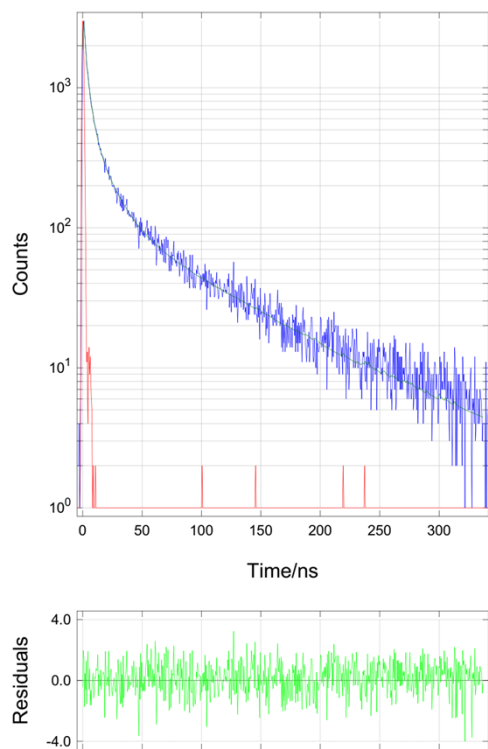


c) 400 nm, DMSO

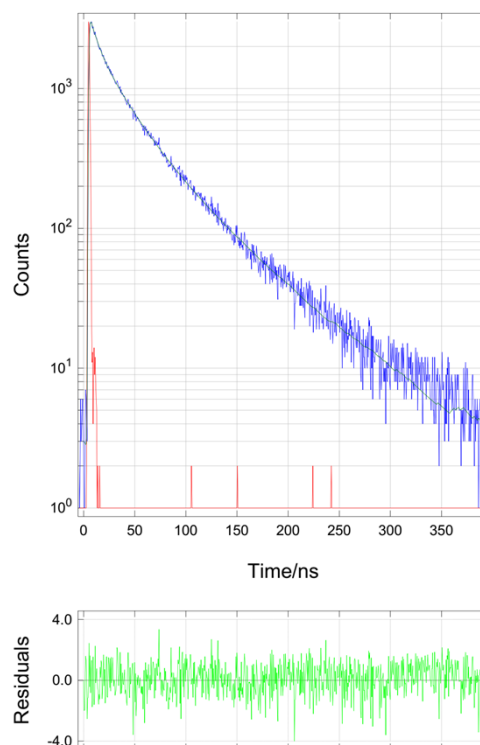


d) 475 nm, DMSO

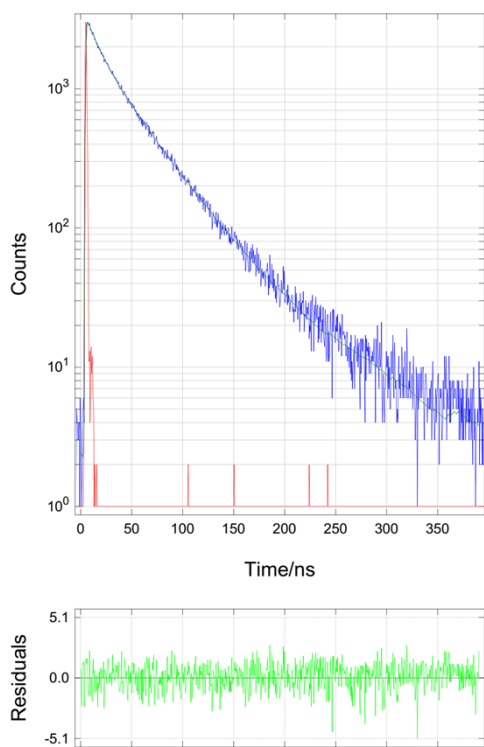
Figure S12. Time resolved fluorescence decay for **2** ($c = 10^{-6}$ M) in water and DMSO at emission wavelengths: 400 and 475 nm. Blue: **2** decay, red: IRF (instrument time response time scan), green: weighted residuals time scan.



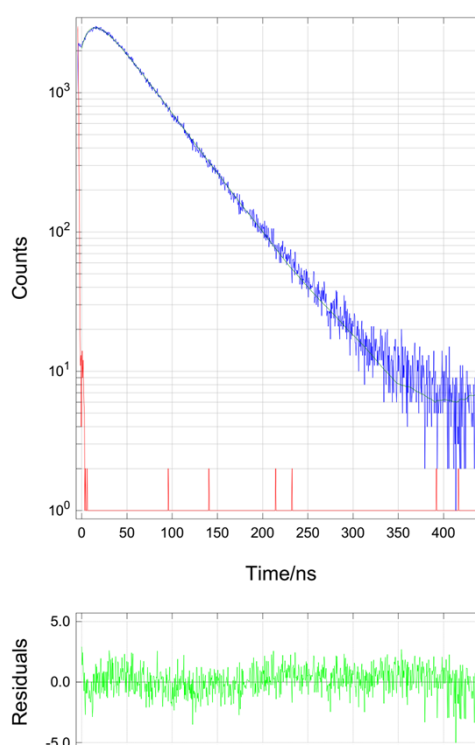
a) 400 nm, water



b) 475 nm, water

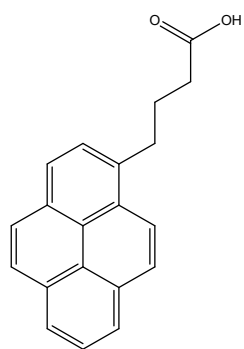


c) 400 nm, DMSO

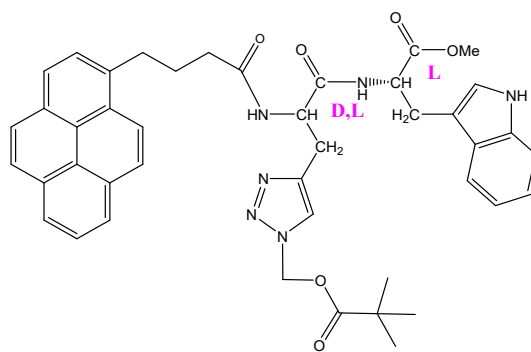


d) 475 nm, DMSO

Figure S13. Time resolved fluorescence decay for **3** ($c = 10^{-6}$ M) in water and DMSO at emission wavelengths: 400 and 475 nm. Blue: **3** decay, red: IRF (instrument time response time scan), green: weighted residuals time scan.



A = 1-pyrenebutyric acid



B = PyrL-Ala(Triazole-R)-Trp

Figure S14. Referent compounds **A** and **B** previously published.¹

¹ I. Krošl, M. Koščak, K. Ribičić, B. Žinić, D. Majhen, K. Božinović and I. Piantanida, Impact of the Histidine-Triazole and Tryptophan-Pyrene Exchange in the WHW Peptide: Cu(II) Binding, DNA/RNA Interactions and Bioactivity, *Int. J. Mol. Sci.* 2022, **23**, 7006.

3. Interactions with DNA and RNA

Table S1. Structural features of selected nucleic acids.^{2,3}

Structure type	Groove width [Å]		Groove depth [Å]	
	major	minor	major	minor
poly A- poly U (A-helix)	3.8	10.9	13.5	2.8
ct-DNA (B-helix)	11.7	5.7	8.5	7.5
(dGdC)_n (B-helix)	13.5	9.5	10.0	7.2
p(dAdT)₂ (B-helix)	11.2	6.3	-	-

² W. Saenger, *Principles of Nucleic Acid Structure*, Springer-Verlag, New York, 1983.

³ C. R. Cantor, P. R. Schimmel, *Biophysical Chemistry*, 1980, **3**, 1109-1181.

3.1. Spectrophotometric titrations with mono- and polynucleotides

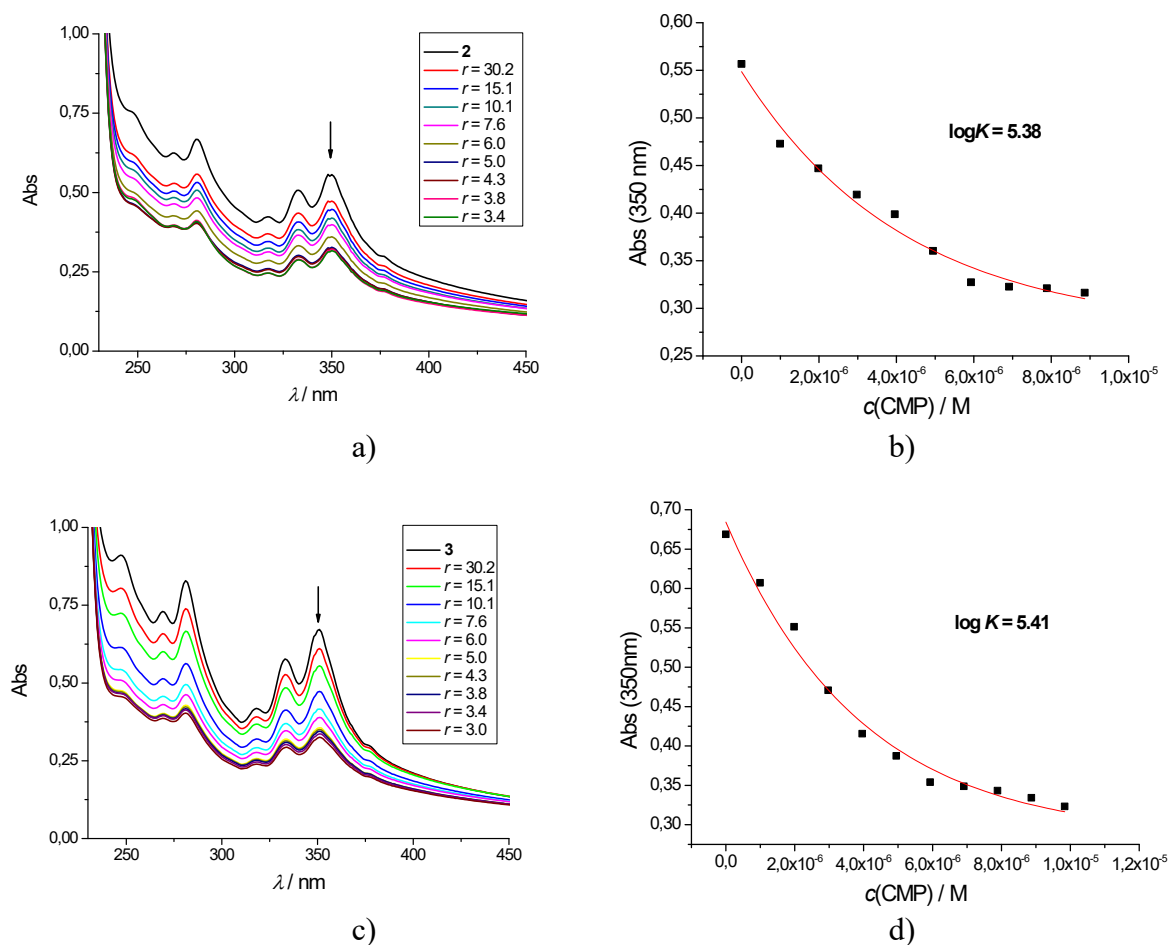


Figure S15. a) Spectrophotometric titration of **2** ($c = 3 \times 10^{-5}$ M) with CMP ($c = 1 \times 10^{-3}$ M) and b) dependence of absorption at $\lambda_{\max} = 350$ nm on $c(\text{CMP})$; c) spectrophotometric titration of **3** ($c = 3 \times 10^{-5}$ M) with CMP ($c = 1 \times 10^{-3}$ M) and d) dependence of absorption at $\lambda_{\max} = 350$ nm on $c(\text{CMP})$. Done in sodium cacodylate buffer (pH=7.0, $I = 0.05$ M); $r = [\text{compound}] / [\text{mononucleotide}]$.

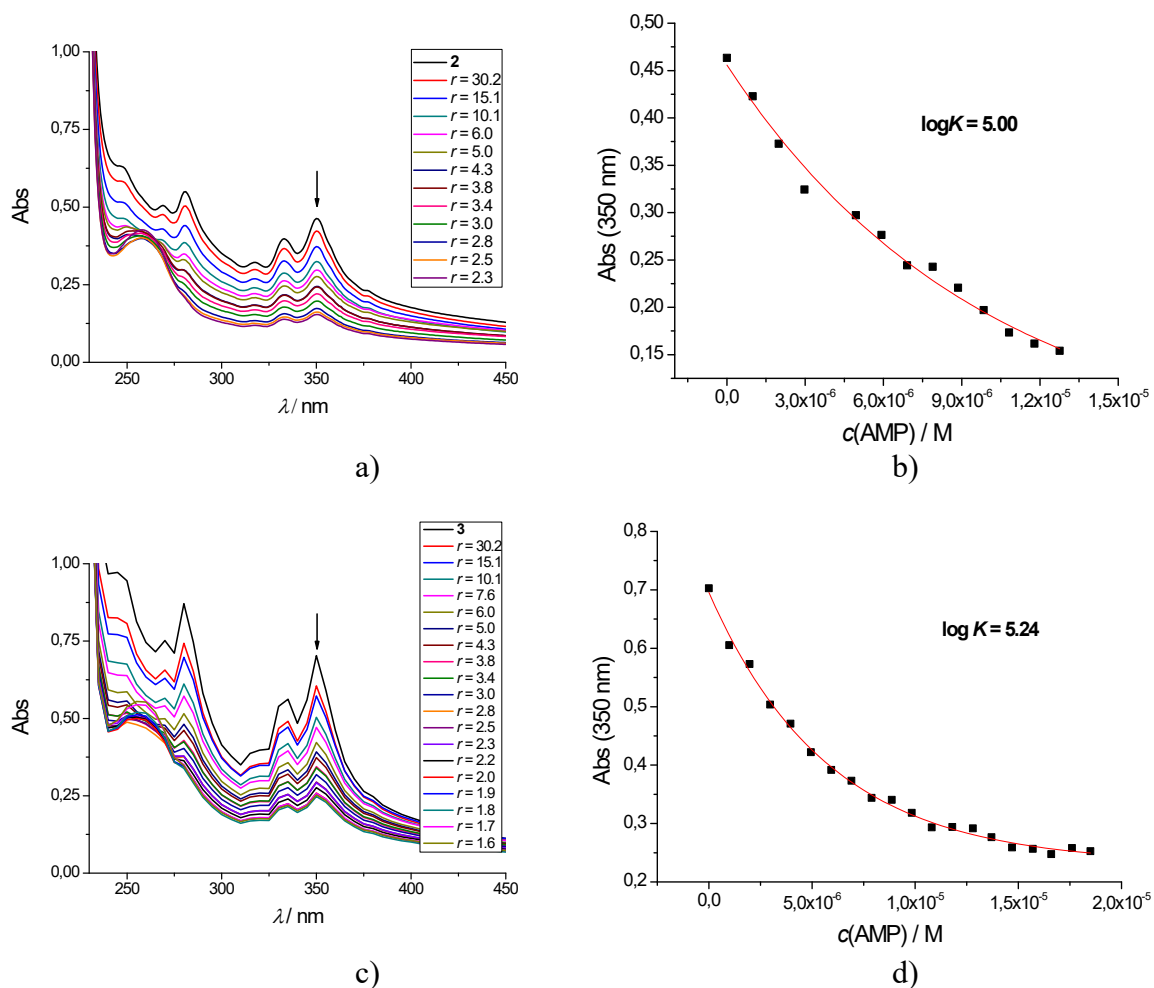


Figure S16. a) Spectrophotometric titration of **2** ($c = 3 \times 10^{-5}$ M) with AMP ($c = 1 \times 10^{-3}$ M) and b) dependence of absorption at $\lambda_{\text{max}} = 350$ nm on $c(\text{AMP})$; c) spectrophotometric titration of **3** ($c = 3 \times 10^{-5}$ M) with AMP ($c = 1 \times 10^{-3}$ M) and d) dependence of absorption at $\lambda_{\text{max}} = 350$ nm on $c(\text{AMP})$. Done in sodium cacodylate buffer (pH=7.0, $I = 0.05$ M); $r = [\text{compound}] / [\text{mononucleotide}]$.

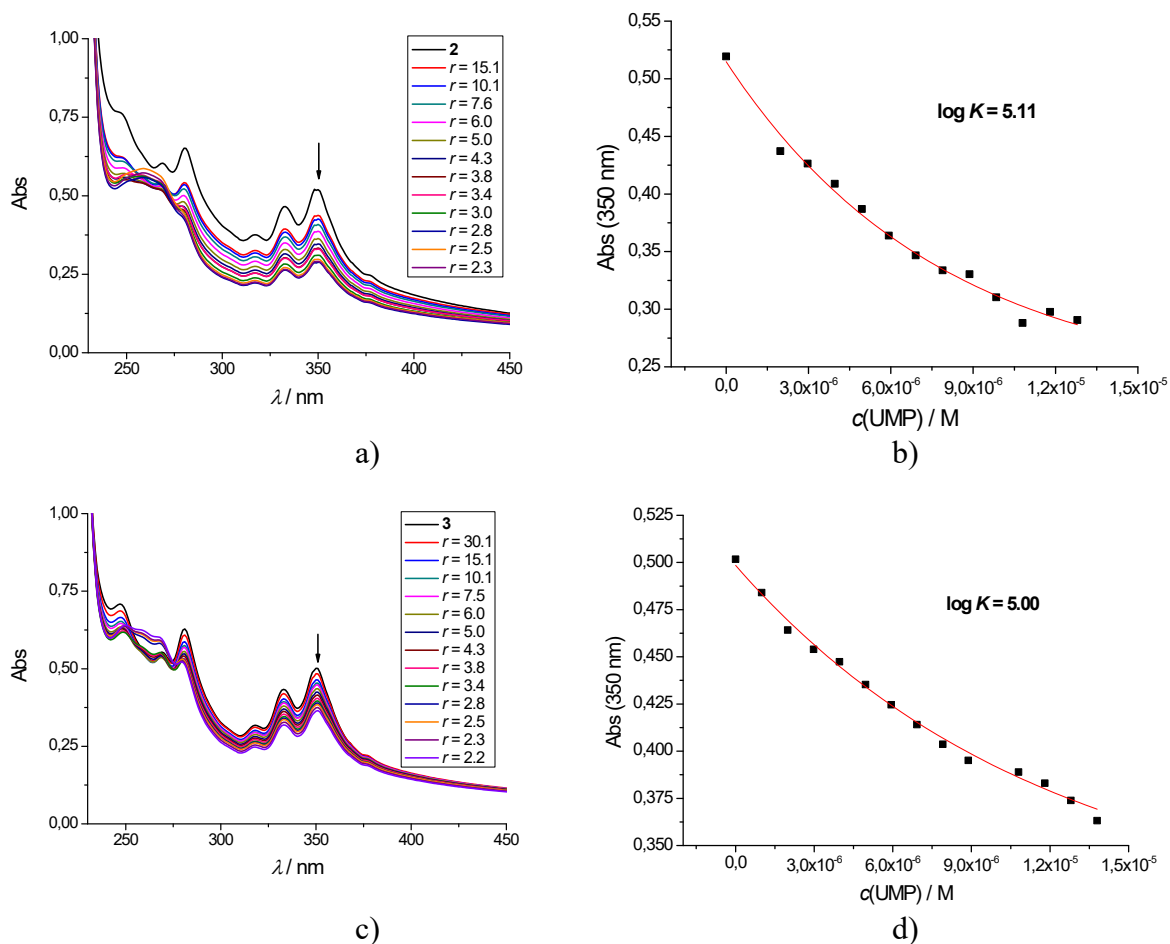


Figure S17. a) Spectrophotometric titration of **2** ($c = 3 \times 10^{-5}$ M) with UMP ($c = 1 \times 10^{-3}$ M) and b) dependence of absorption at $\lambda_{\max} = 350$ nm on $c(\text{UMP})$; c) spectrophotometric titration of **3** ($c = 3 \times 10^{-5}$ M) with UMP ($c = 1 \times 10^{-3}$ M) and d) dependence of absorption at $\lambda_{\max} = 350$ nm on $c(\text{UMP})$. Done in sodium cacodylate buffer (pH=7.0, $I = 0.05$ M); $r = [\text{compound}] / [\text{mononucleotide}]$.

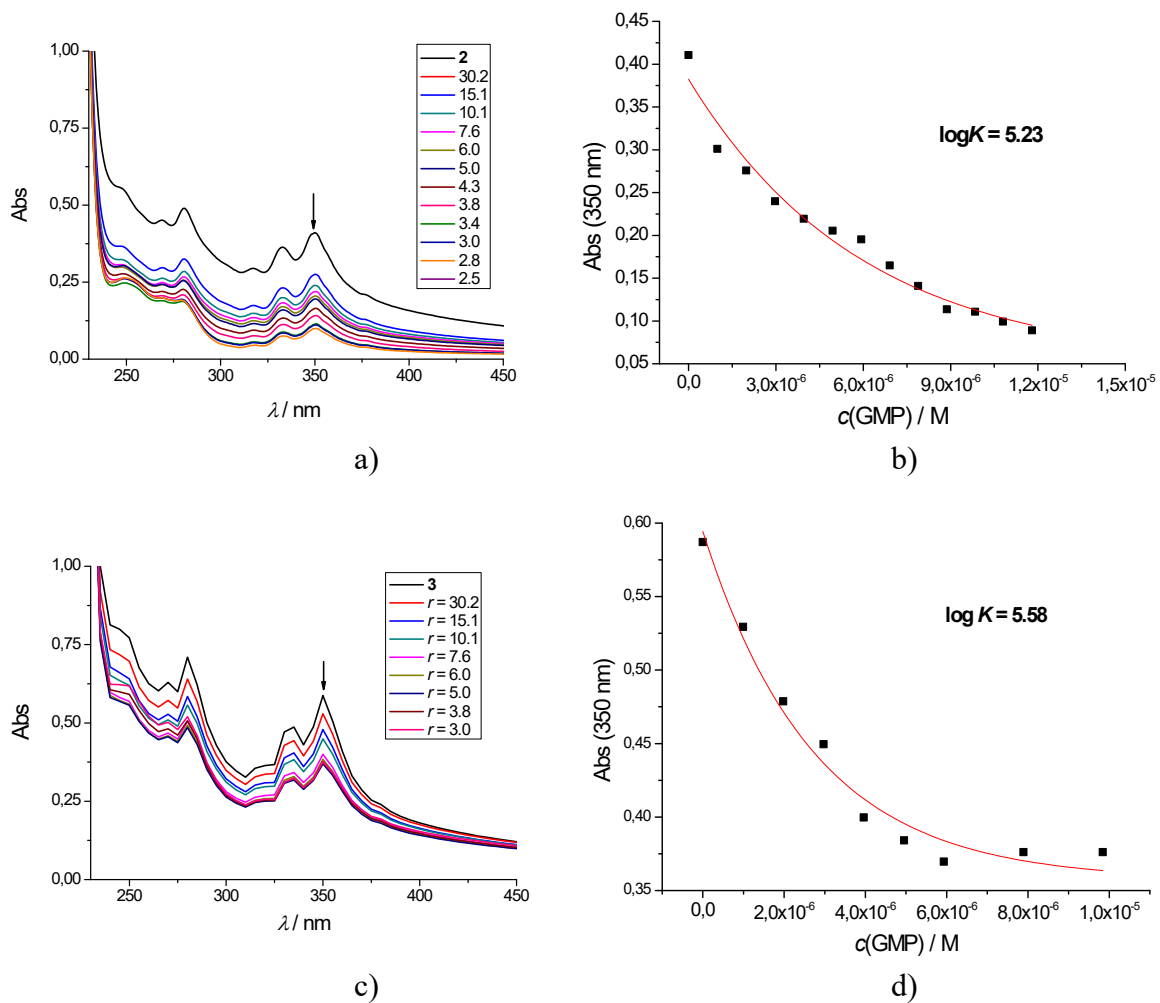


Figure S18. a) Spectrophotometric titration of **2** ($c = 3 \times 10^{-5}$ M) with GMP ($c = 1 \times 10^{-3}$ M) and b) dependence of absorption at $\lambda_{\text{max}} = 350$ nm on $c(\text{GMP})$; c) spectrophotometric titration of **3** ($c = 3 \times 10^{-5}$ M) with GMP ($c = 1 \times 10^{-3}$ M) and d) dependence of absorption at $\lambda_{\text{max}} = 350$ nm on $c(\text{GMP})$. Done in sodium cacodylate buffer (pH=7.0, $I = 0.05$ M); $r = [\text{compound}] / [\text{mononucleotide}]$.

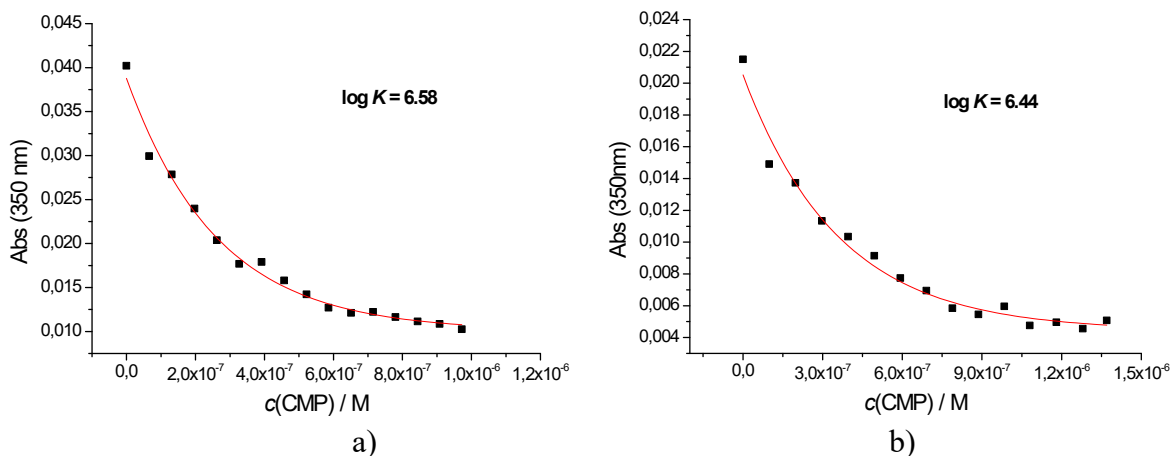


Figure S19. a) Absorption dependence of **2** ($c = 2 \times 10^{-6} \text{ M}$) on concentration of CMP ($c = 6.67 \times 10^{-5} \text{ M}$) at $\lambda_{\text{max}} = 350 \text{ nm}$ on $c(\text{CMP})$; b) Absorption dependence of **3** ($c = 3 \times 10^{-6} \text{ M}$) on concentration of CMP ($c = 1 \times 10^{-4} \text{ M}$) at $\lambda_{\text{max}} = 350 \text{ nm}$ on $c(\text{CMP})$. Done in sodium cacodylate buffer (pH=7.0, $I = 0.05 \text{ M}$).

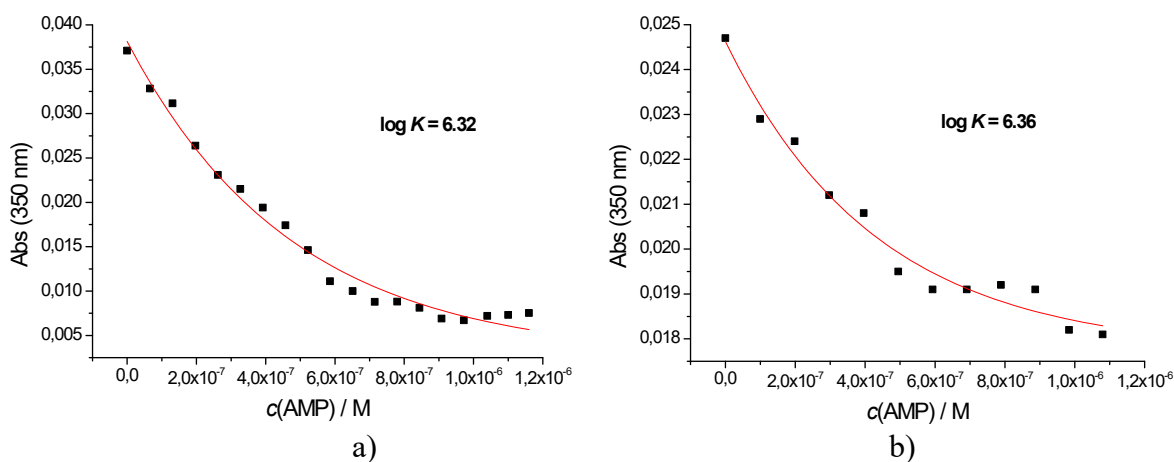


Figure S20. a) Absorption dependence of **2** ($c = 2 \times 10^{-6} \text{ M}$) on concentration of AMP ($c = 6.67 \times 10^{-5} \text{ M}$) at $\lambda_{\text{max}} = 350 \text{ nm}$ on $c(\text{AMP})$; b) Absorption dependence of **3** ($c = 3 \times 10^{-6} \text{ M}$) on concentration of AMP ($c = 1 \times 10^{-4} \text{ M}$) at $\lambda_{\text{max}} = 350 \text{ nm}$ on $c(\text{AMP})$. Done in sodium cacodylate buffer (pH=7.0, $I = 0.05 \text{ M}$).

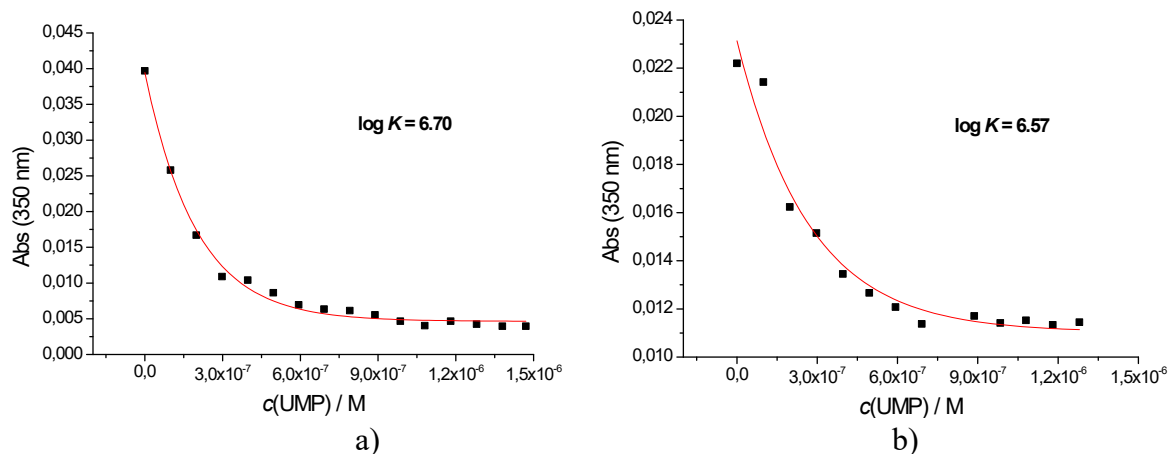


Figure S21. a) Absorption dependence of **2** ($c = 2 \times 10^{-6}$ M) on concentration of UMP ($c = 1 \times 10^{-4}$ M) at $\lambda_{\max} = 350$ nm on $c(\text{UMP})$; b) Absorption dependence of **3** ($c = 3 \times 10^{-6}$ M) on concentration of UMP ($c = 1 \times 10^{-4}$ M) at $\lambda_{\max} = 350$ nm on $c(\text{UMP})$. Done in sodium cacodylate buffer (pH=7.0, $I = 0.05$ M).

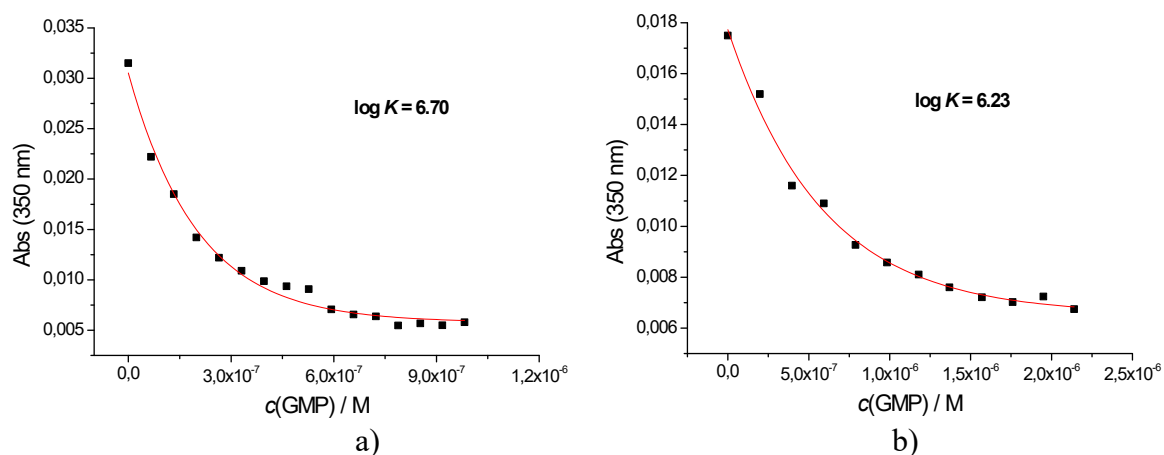
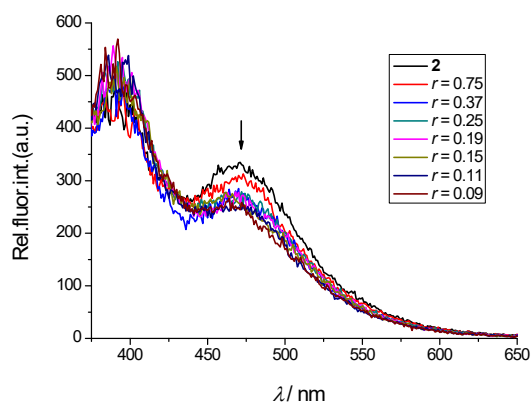
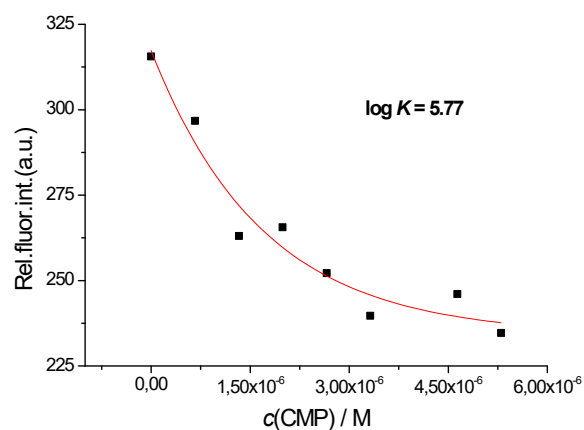


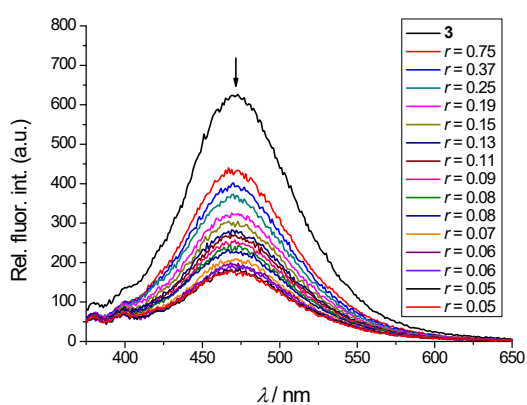
Figure S22. a) Absorption dependence of **2** ($c = 2 \times 10^{-6}$ M) on concentration of GMP ($c = 6.67 \times 10^{-5}$ M) at $\lambda_{\max} = 350$ nm on $c(\text{GMP})$; b) Absorption dependence of **3** ($c = 3 \times 10^{-6}$ M) on concentration of GMP ($c = 1 \times 10^{-4}$ M) at $\lambda_{\max} = 350$ nm on $c(\text{GMP})$. Done in sodium cacodylate buffer (pH=7.0, $I = 0.05$ M).



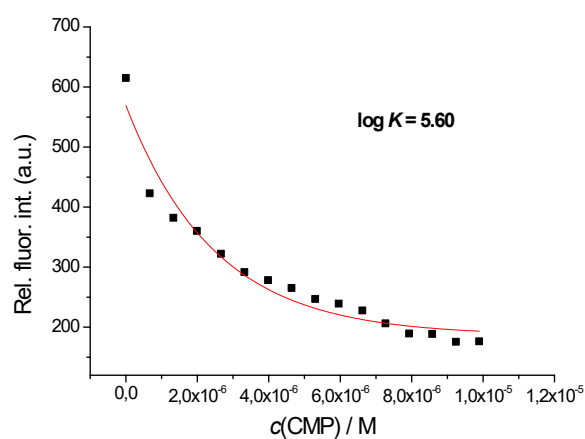
a)



b)

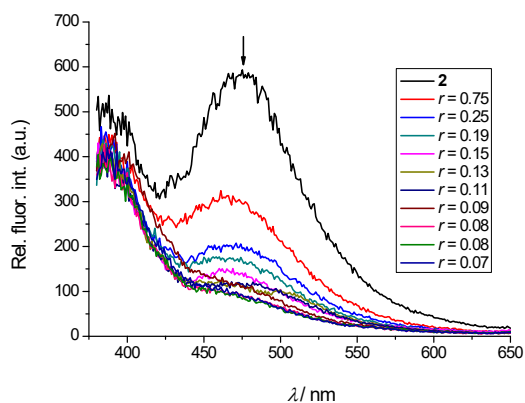


c)

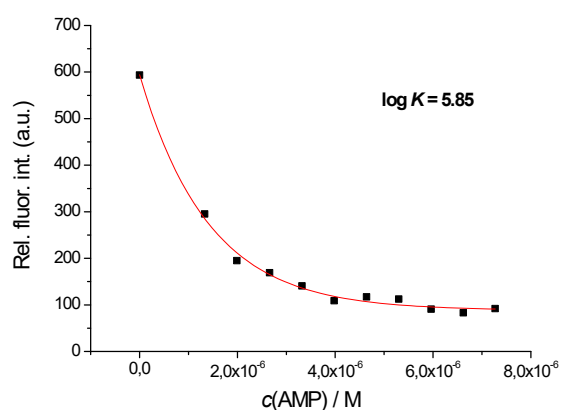


d)

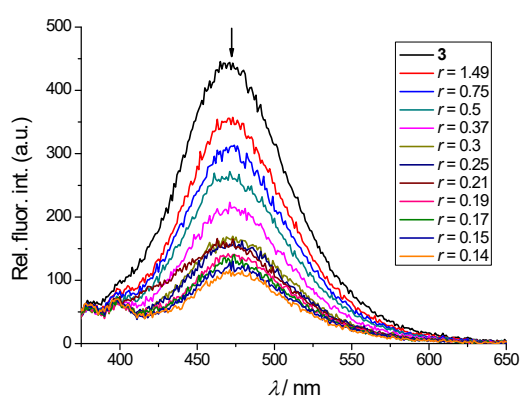
Figure S23. a) Fluorimetric titration of **2** ($c = 5 \times 10^{-7}$ M; $\lambda_{\text{exc}} = 350$ nm) with CMP ($c = 1 \times 10^{-3}$ M) and b) dependence of fluorescence at $\lambda_{\text{max}} = 475$ nm on $c(\text{CMP})$; c) fluorimetric titration of **3** ($c = 5 \times 10^{-7}$ M; $\lambda_{\text{exc}} = 350$ nm) with CMP ($c = 1 \times 10^{-3}$ M) and d) dependence of fluorescence at $\lambda_{\text{max}} = 475$ nm on $c(\text{CMP})$. Done in sodium cacodylate buffer (pH=7.0, $I = 0.05$ M); $r = [\text{compound}] / [\text{mononucleotide}]$.



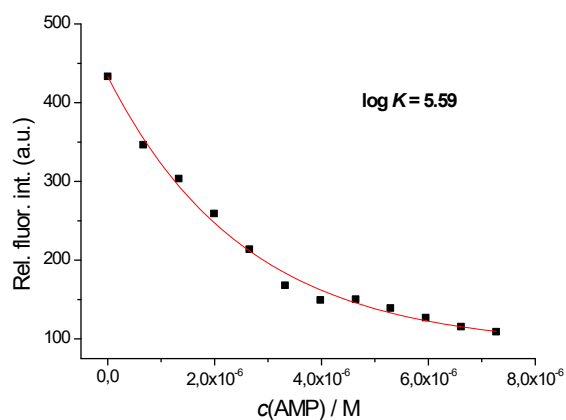
a)



b)

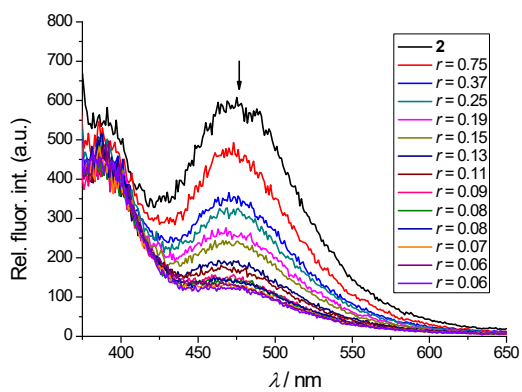


c)

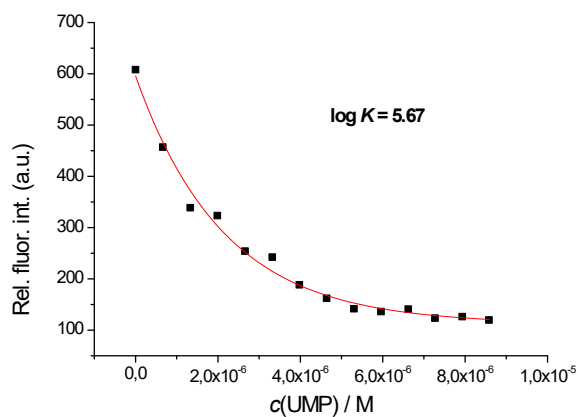


d)

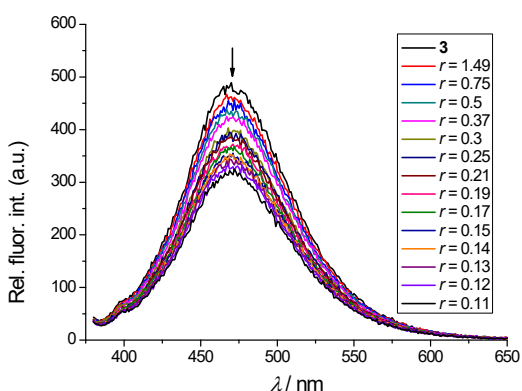
Figure S24. a) Fluorimetric titration of **2** ($c = 5 \times 10^{-7}$ M; $\lambda_{\text{exc}} = 350$ nm) with AMP ($c = 1 \times 10^{-3}$ M) and b) dependence of fluorescence at $\lambda_{\text{max}} = 475$ nm on $c(\text{AMP})$; c) fluorimetric titration of **3** ($c = 1 \times 10^{-6}$ M; $\lambda_{\text{exc}} = 350$ nm) with AMP ($c = 1 \times 10^{-3}$ M) and d) dependence of fluorescence at $\lambda_{\text{max}} = 475$ nm on $c(\text{AMP})$. Done in sodium cacodylate buffer (pH=7.0, $I = 0.05$ M); $r = [\text{compound}] / [\text{mononucleotide}]$.



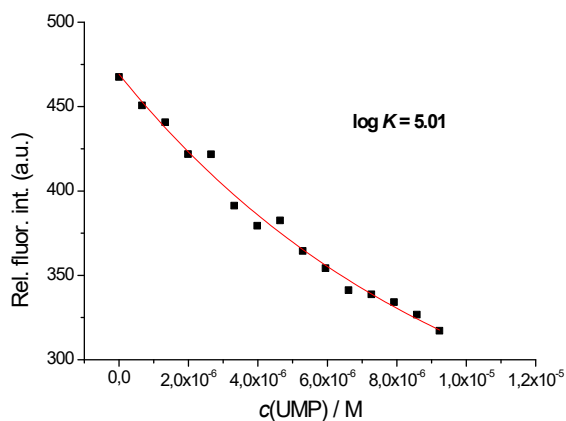
a)



b)



c)



d)

Figure S25. a) Fluorimetric titration of **2** ($c = 5 \times 10^{-7}$ M; $\lambda_{\text{exc}} = 350$ nm) with UMP ($c = 1 \times 10^{-3}$ M) and b) dependence of fluorescence at $\lambda_{\text{max}} = 475$ nm on $c(\text{UMP})$; c) fluorimetric titration of **3** ($c = 1 \times 10^{-6}$ M; $\lambda_{\text{exc}} = 350$ nm) with UMP ($c = 1 \times 10^{-3}$ M) and d) dependence of fluorescence at $\lambda_{\text{max}} = 475$ nm on $c(\text{UMP})$. Done in sodium cacodylate buffer (pH=7.0, $I = 0.05$ M); $r = [\text{compound}] / [\text{mononucleotide}]$.

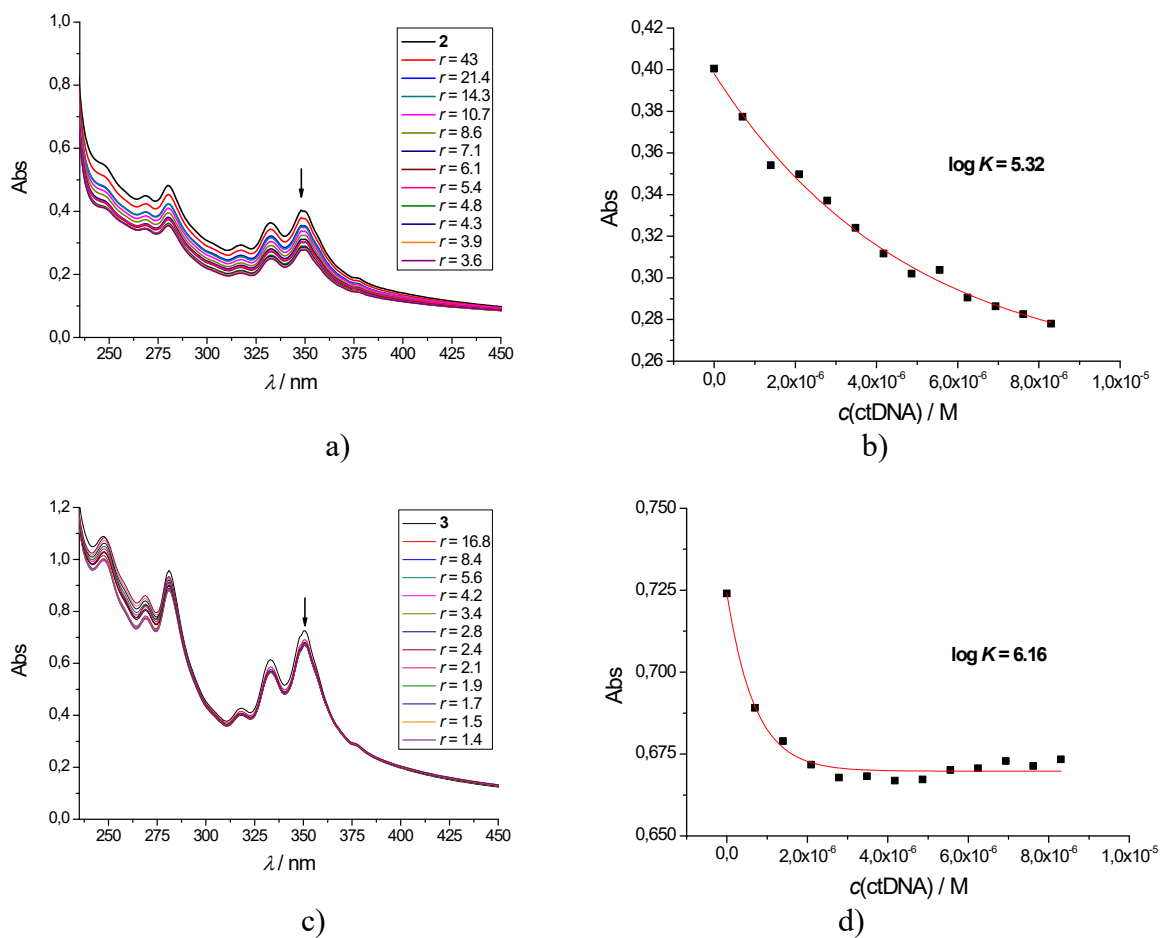
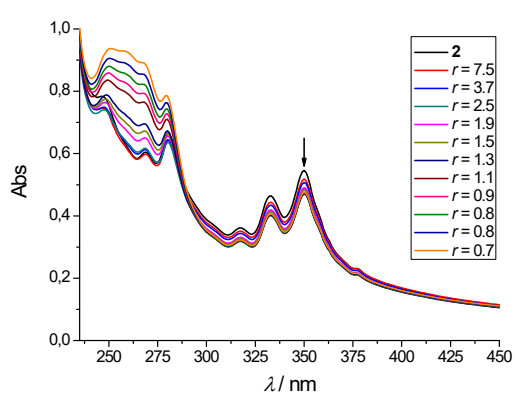
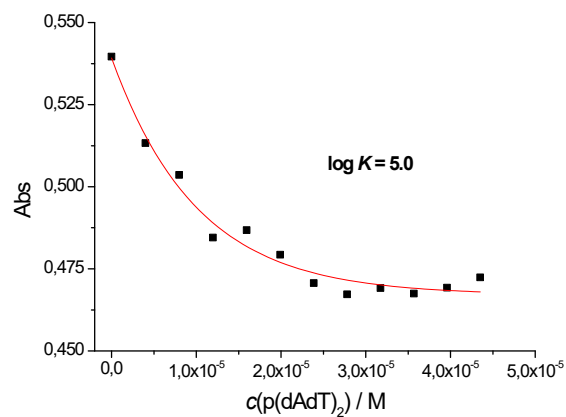


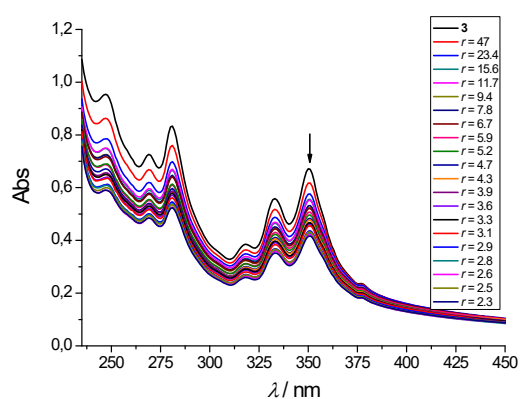
Figure S26. a) Spectrophotometric titration of **2** ($c = 3 \times 10^{-5} \text{ M}$) with ctDNA ($c = 7 \times 10^{-4} \text{ M}$) and b) dependence of absorption at $\lambda_{\text{max}} = 350 \text{ nm}$ on $c(\text{ctDNA})$; c) spectrophotometric titration of **3** ($c = 3 \times 10^{-5} \text{ M}$) with ctDNA ($c = 1.79 \times 10^{-3} \text{ M}$) and d) dependence of absorption at $\lambda_{\text{max}} = 350 \text{ nm}$ on $c(\text{ctDNA})$. Done in sodium cacodylate buffer (pH=7.0, $I = 0.05 \text{ M}$); $r = [\text{compound}] / [\text{DNA/RNA}]$.



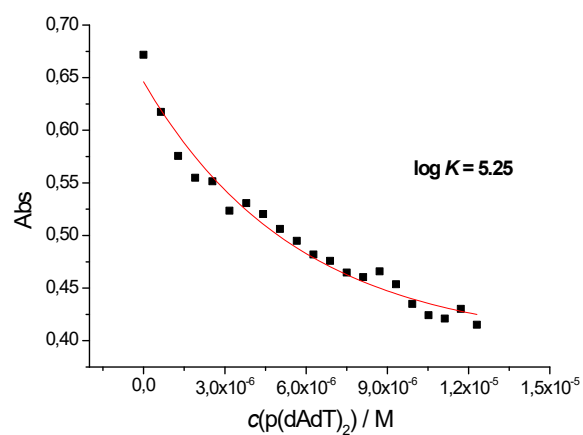
a)



b)

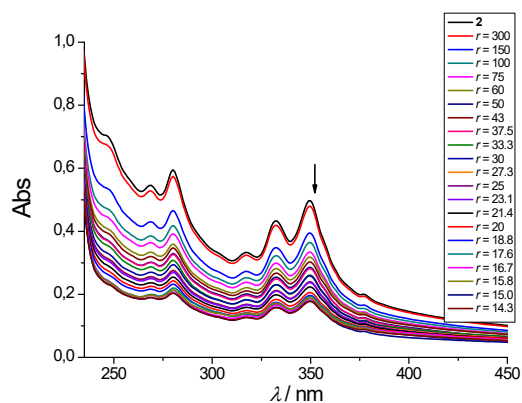


c)

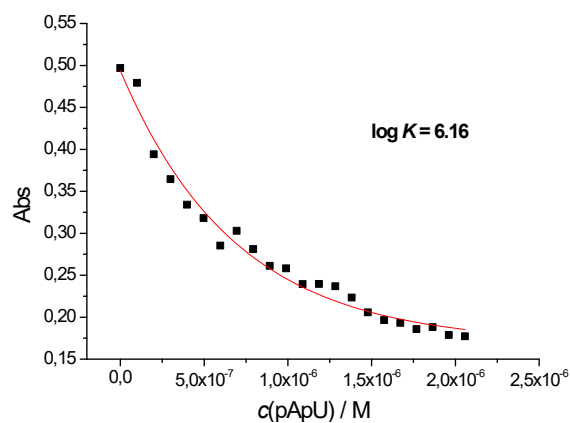


d)

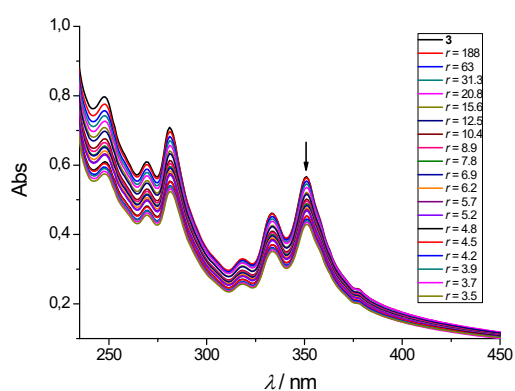
Figure S27. a) Spectrophotometric titration of **2** ($c = 3 \times 10^{-5}$ M) with $p(dAdT)_2$ ($c = 4 \times 10^{-3}$ M) and b) dependence of absorbance at $\lambda_{\max} = 350$ nm on $c(p(dAdT)_2)$; c) spectrophotometric titration of **3** ($c = 3 \times 10^{-5}$ M) with $p(dAdT)_2$ ($c = 3.2 \times 10^{-4}$ M) and d) dependence of absorbance at $\lambda_{\max} = 350$ nm on $c(p(dAdT)_2)$. Done in sodium cacodylate buffer (pH=7.0, $I = 0.05$ M); $r = [\text{compound}] / [\text{DNA/RNA}]$.



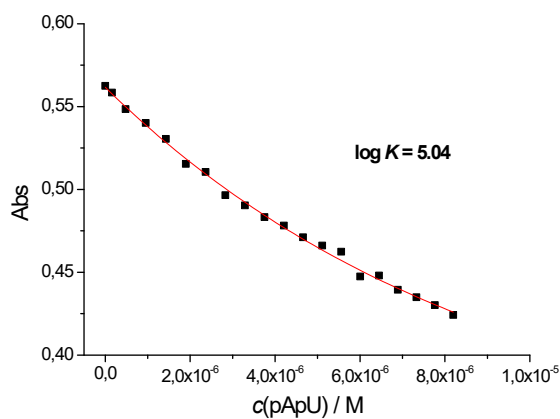
a)



b)



c)



d)

Figure S28. a) Spectrophotometric titration of **2** ($c = 3 \times 10^{-5}$ M) with pApU ($c = 1 \times 10^{-4}$ M) and b) dependence of absorbance at $\lambda_{\max} = 350$ nm on $c(\text{pApU})$; c) spectrophotometric titration of **3** ($c = 3 \times 10^{-5}$ M) with pApU ($c = 1.6 \times 10^{-4}$ M) and d) dependence of absorbance at $\lambda_{\max} = 350$ nm on $c(\text{pApU})$. Done in sodium cacodylate buffer (pH=7.0, $I = 0.05$ M); $r = [\text{compound}] / [\text{DNA/RNA}]$.

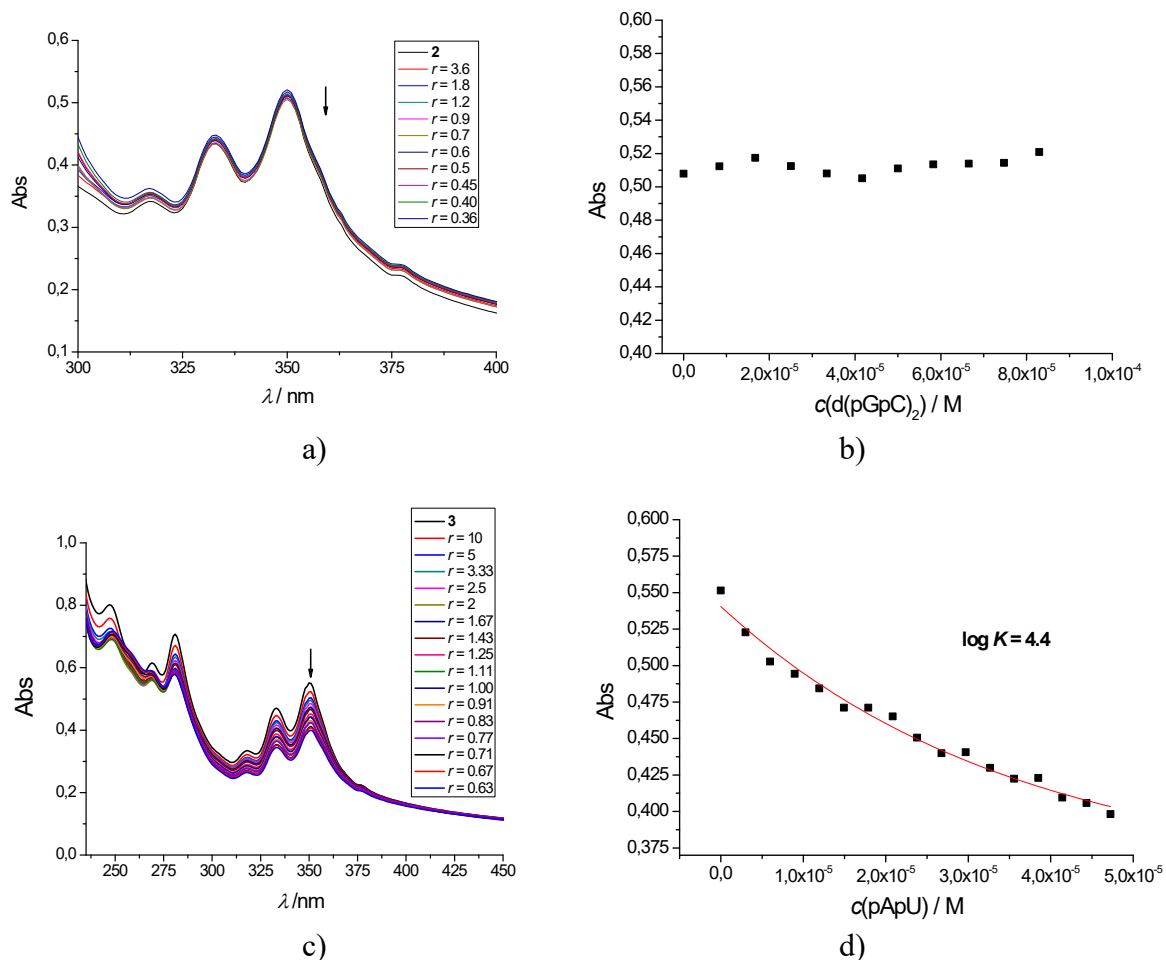


Figure S29. a) Spectrophotometric titration of **2** ($c = 3 \times 10^{-5}$ M) with $p(dGdC)_2$ ($c = 8.38 \times 10^{-3}$ M) and b) dependence of absorption at $\lambda_{max} = 350$ nm on $c(p(dGdC)_2)$; c) spectrophotometric titration of **3** ($c = 3 \times 10^{-5}$ M) with $p(dGdC)_2$ ($c = 3 \times 10^{-3}$ M) and d) dependence of absorption at $\lambda_{max} = 350$ nm on $c(p(dGdC)_2)$. Done in sodium cacodylate buffer (pH=7.0, $I = 0.05$ M); $r = [\text{compound}] / [\text{DNA/RNA}]$.

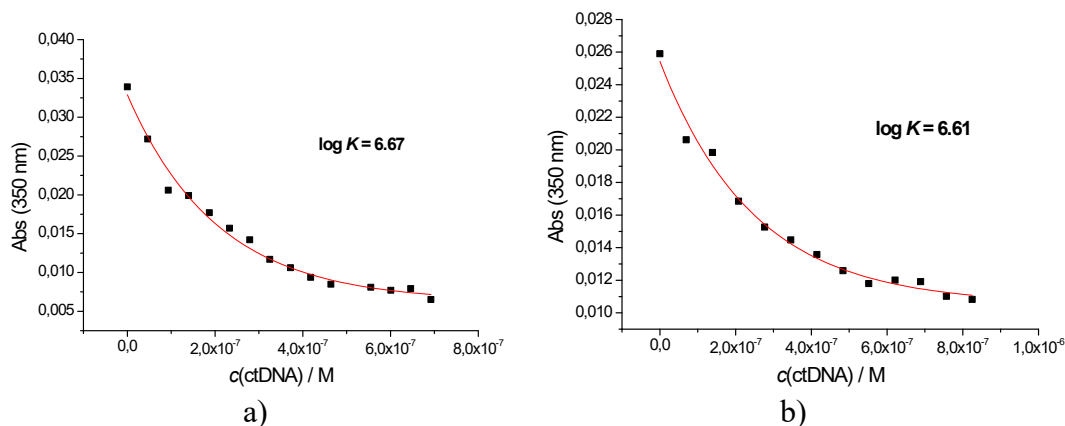


Figure S30. a) Absorption dependence of **2** ($c = 2 \times 10^{-6}$ M) on concentration of ctDNA ($c = 4.7 \times 10^{-5}$ M) at $\lambda_{\max} = 350$ nm; b) Absorption dependence of **3** ($c = 3 \times 10^{-6}$ M) on concentration of ctDNA ($c = 7 \times 10^{-5}$ M) at $\lambda_{\max} = 350$ nm on $c(\text{ctDNA})$. Done in sodium cacodylate buffer (pH=7.0, $I = 0.05$ M); $r = [\text{compound}] / [\text{DNA/RNA}]$.

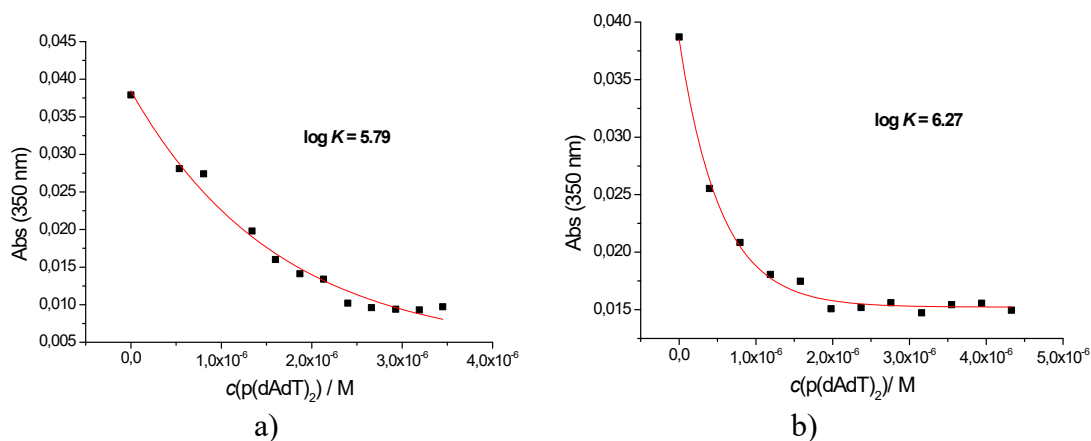


Figure S31. a) Absorption dependence of **2** ($c = 2 \times 10^{-6}$ M) on concentration of p(dAdT)₂ ($c = 2.7 \times 10^{-4}$ M) at $\lambda_{\max} = 350$ nm on $c(\text{p(dAdT)}_2)$; b) Absorption dependence of **3** ($c = 3 \times 10^{-6}$ M) on concentration of p(dAdT)₂ ($c = 4 \times 10^{-4}$ M) at $\lambda_{\max} = 350$ nm on $c(\text{p(dAdT)}_2)$. Done in sodium cacodylate buffer (pH=7.0, $I = 0.05$ M); $r = [\text{compound}] / [\text{DNA/RNA}]$.

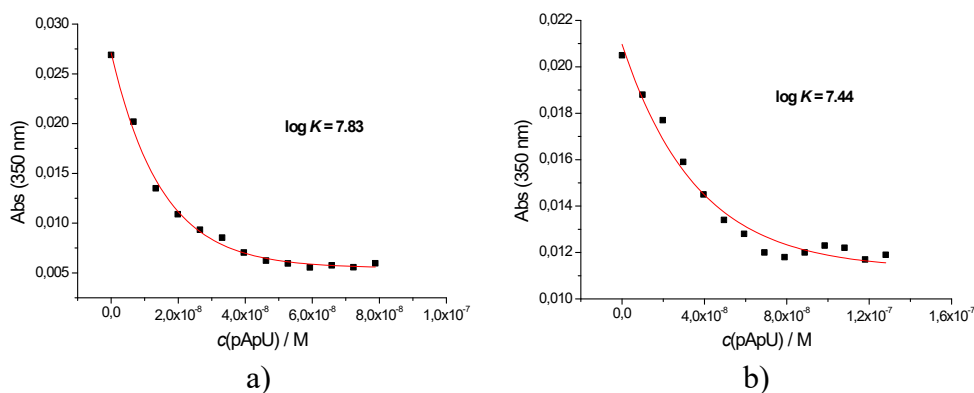


Figure S32. a) Absorption dependence of **2** ($c = 2 \times 10^{-6}$ M) on concentration of pApU ($c = 6.67 \times 10^{-6}$ M) at $\lambda_{\max} = 350$ nm on $c(\text{pApU})$; b) Absorption dependence of **3** ($c = 3 \times 10^{-6}$ M) on concentration of pApU ($c = 1 \times 10^{-5}$ M) at $\lambda_{\max} = 350$ nm on $c(\text{pApU})$. Done in sodium cacodylate buffer (pH=7.0, $I = 0.05$ M); $r = [\text{compound}] / [\text{DNA/RNA}]$.

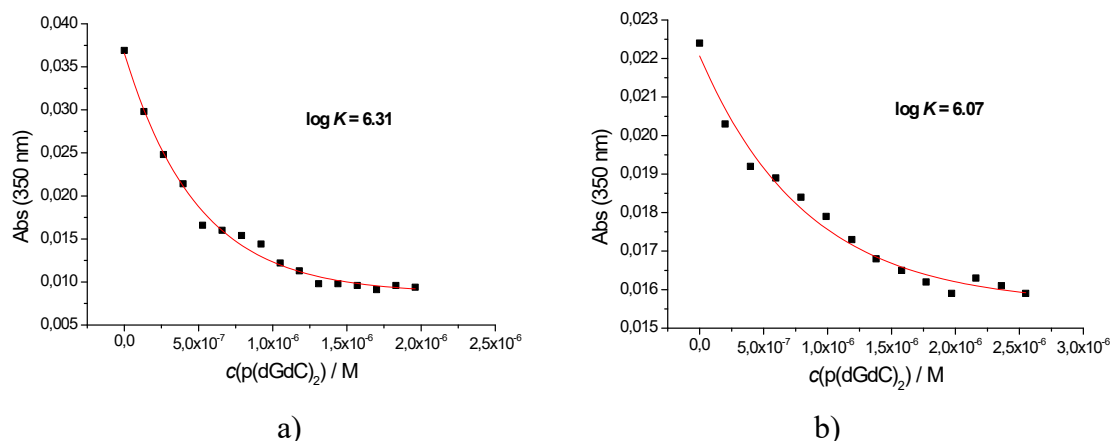


Figure S33. a) Absorption dependence of **2** ($c = 2 \times 10^{-6}$ M) on concentration of p(dGdC)₂ ($c = 1.33 \times 10^{-4}$ M) at $\lambda_{\max} = 350$ nm on $c(\text{p(dGdC)}_2)$; b) Absorption dependence of **3** ($c = 3 \times 10^{-6}$ M) on concentration of p(dGdC)₂ ($c = 2 \times 10^{-4}$ M) at $\lambda_{\max} = 350$ nm on $c(\text{p(dGdC)}_2)$. Done in sodium cacodylate buffer (pH=7.0, $I = 0.05$ M); $r = [\text{compound}] / [\text{DNA/RNA}]$.

Table S2. Binding constants (^alog K) for **2** and **3** with mononucleotides and ds-DNA/ds-RNA determined spectrophotometrically. Done in sodium cacodylate buffer (pH = 7.0, $I = 0.05$ M).

	2	3
CMP	5.4	5.4
AMP	5.0	5.2
UMP	5.1	5.0
GMP	5.2	5.6
ctDNA	6.7 ^b	6.6 ^b
p(dAdT) ₂	5.8 ^b	6.3 ^b
pApU	7.8 ^b	7.4 ^b
p(dGdC) ₂	6.3 ^b	6.1 ^b

^a The best fit of experimental data was obtained for 1:1 stoichiometry of dye/NMP complex or for DNA/RNA by processing of titration data by means of Scatchard equation gave values of ratio $n[\text{bound dye}] / [\text{DNA/RNA}] = 0.1$ and 0.2 , for easier comparison all log K values were re-calculated for fixed $n = 0.2$.

^b UV-Vis titration performed at 350 nm.

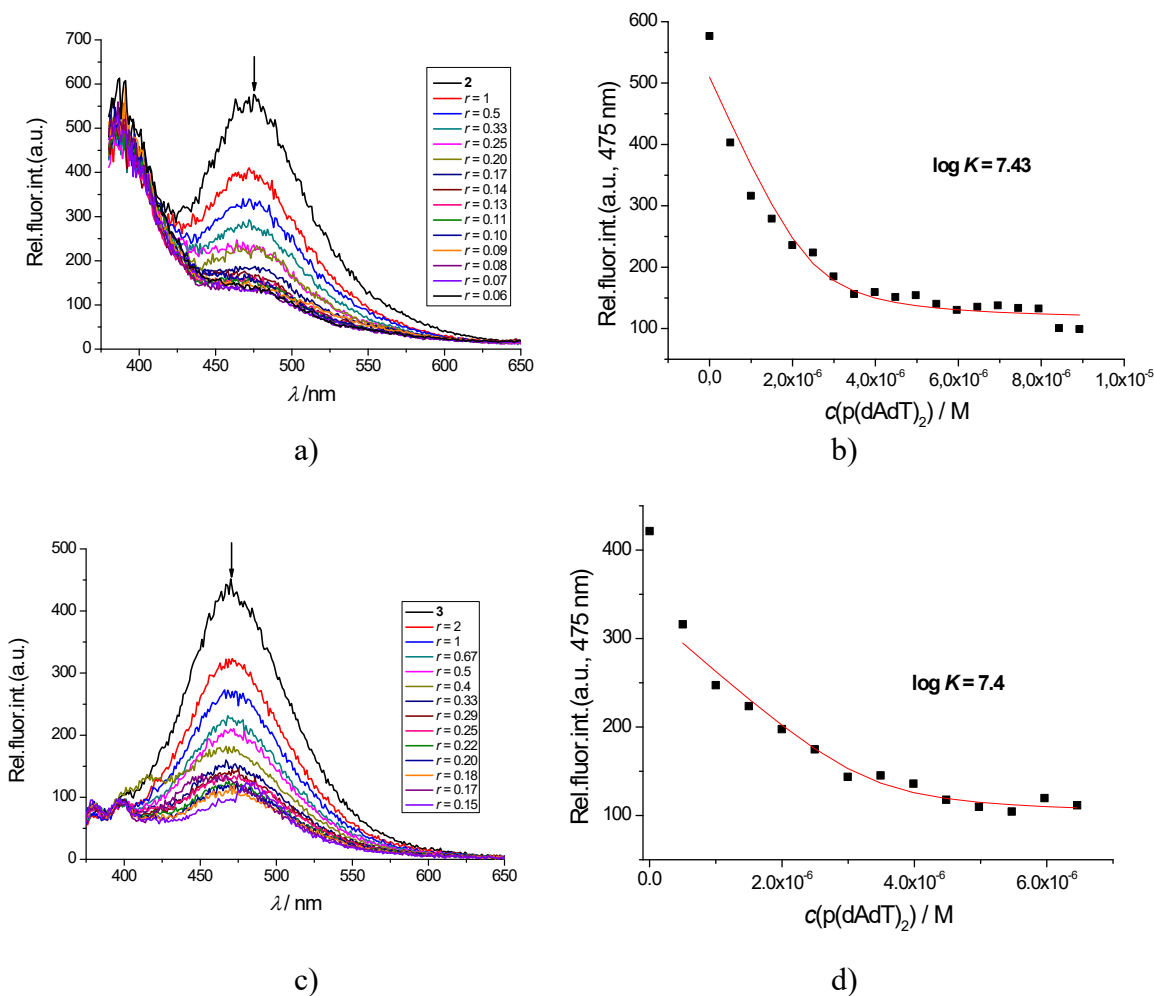


Figure S34. a) Fluorimetric titration of **2** ($c = 5 \times 10^{-7}$ M; $\lambda_{\text{exc}} = 350$ nm) with $p(\text{dAdT})_2$ ($c = 1 \times 10^{-3}$ M) and b) dependence of fluorescence at $\lambda_{\text{max}} = 475$ nm on $c(p(\text{dAdT})_2)$; c) fluorimetric titration of **3** ($c = 1 \times 10^{-6}$ M; $\lambda_{\text{exc}} = 350$ nm) with $p(\text{dAdT})_2$ ($c = 1 \times 10^{-3}$ M) and d) dependence of fluorescence at $\lambda_{\text{max}} = 475$ nm on $c(p(\text{dAdT})_2)$. Done in sodium cacodylate buffer (pH=7.0, $I = 0.05$ M); $r = [\text{compound}] / [\text{DNA/RNA}]$.

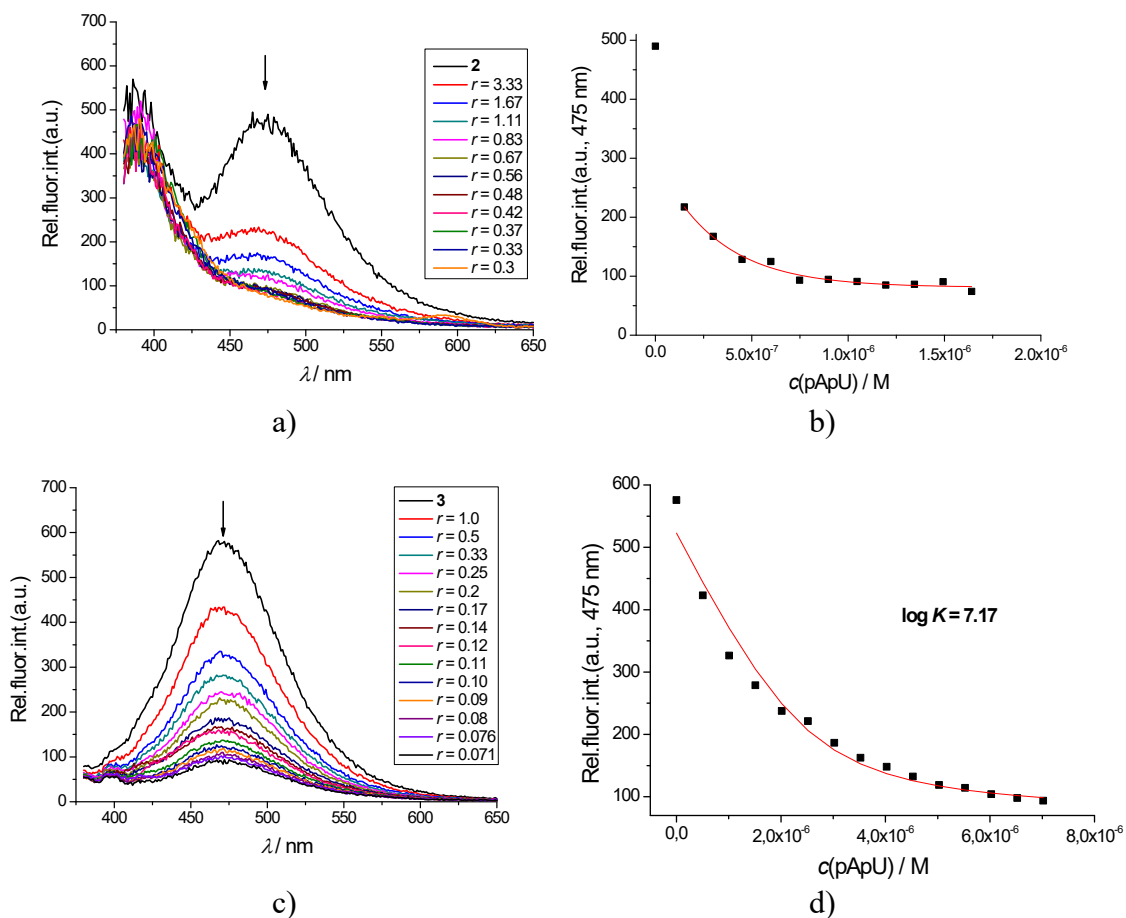
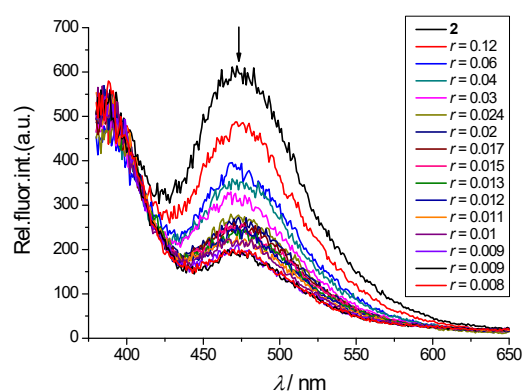
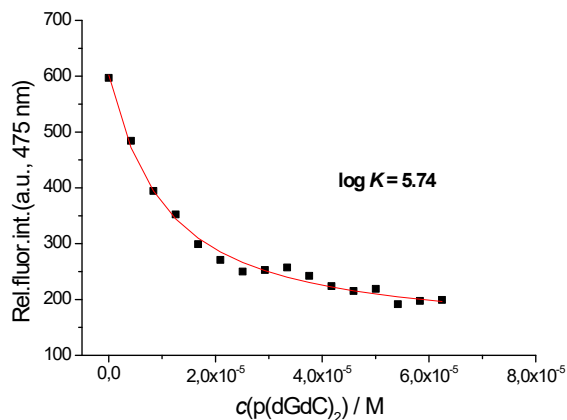


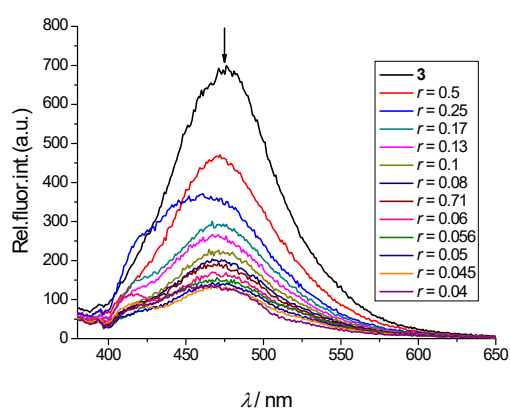
Figure S35. a) Fluorimetric titration of **2** ($c = 5 \times 10^{-7} \text{ M}$; $\lambda_{\text{exc}} = 350 \text{ nm}$) with pApU ($c = 3 \times 10^{-4} \text{ M}$) and b) dependence of fluorescence at $\lambda_{\text{max}} = 475 \text{ nm}$ on $c(\text{pApU})$; c) fluorimetric titration of **3** ($c = 5 \times 10^{-7} \text{ M}$; $\lambda_{\text{exc}} = 350 \text{ nm}$) with pApU ($c = 1.01 \times 10^{-3} \text{ M}$) and d) dependence of fluorescence at $\lambda_{\text{max}} = 475 \text{ nm}$ on $c(\text{pApU})$. Done in sodium cacodylate buffer (pH=7.0, $I = 0.05 \text{ M}$); $r = [\text{compound}] / [\text{DNA/RNA}]$.



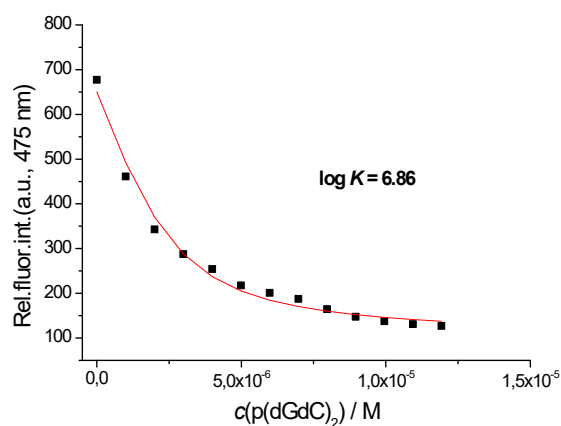
a)



b)



c)



d)

Figure S36. a) Fluorimetric titration of **2** ($c = 5 \times 10^{-7}$ M; $\lambda_{\text{exc}} = 350$ nm) with p(dGdC)_2 ($c = 8.39 \times 10^{-3}$ M) and b) dependence of fluorescence at $\lambda_{\text{max}} = 475$ nm on $c(\text{p(dGdC)}_2)$; c) fluorimetric titration of **3** ($c = 5 \times 10^{-7}$ M; $\lambda_{\text{exc}} = 350$ nm) with p(dGdC)_2 ($c = 2 \times 10^{-3}$ M) and d) dependence of fluorescence at $\lambda_{\text{max}} = 475$ nm on $c(\text{p(dGdC)}_2)$. Done in sodium cacodylate buffer (pH=7.0, $I = 0.05$ M); $r = [\text{compound}] / [\text{DNA/RNA}]$.

3.2. Circular dichroism (CD) experiments

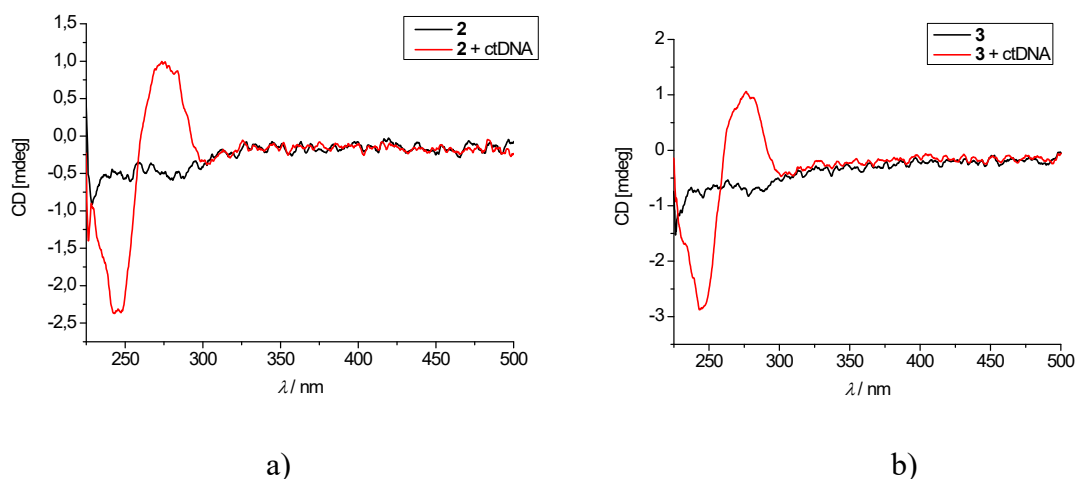


Figure S37. CD spectra of: a) **2** and b) **3** ($c = 1 \times 10^{-5}$ M) and after addition of ctDNA ($c = 3 \times 10^{-5}$ M) at molar ratio $r = 3$ ($r = [\text{compound}] / [\text{polynucleotide}]$). Done at pH = 7.0, sodium cacodylate buffer, $I = 0.05$ M.

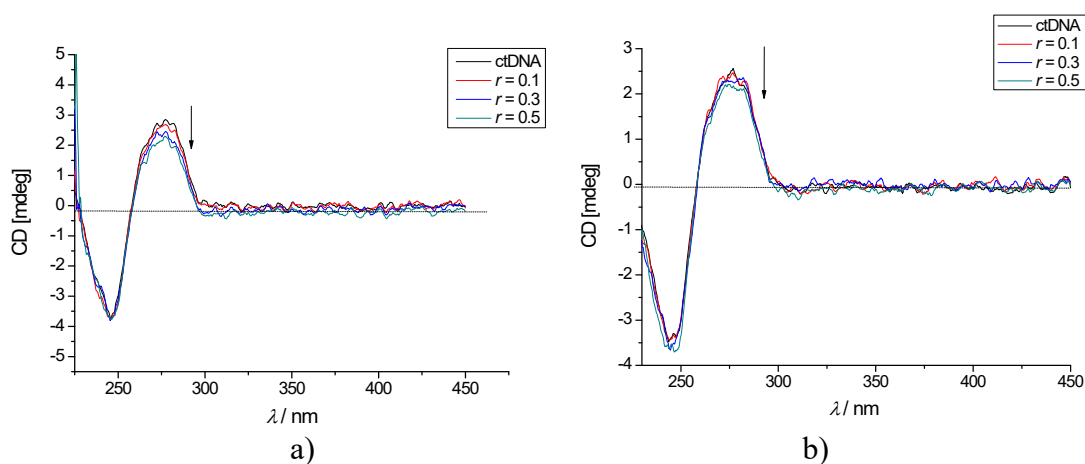


Figure S38. CD titration of ctDNA ($c = 3 \times 10^{-5}$ M) with: a) **2** ($c = 5 \times 10^{-3}$ M) and b) **3** ($c = 5 \times 10^{-3}$ M) at different ratio. Done in sodium cacodylate buffer (pH = 7.0, $I = 0.05$ M); $r = [\text{compound}] / [\text{DNA/RNA}]$.

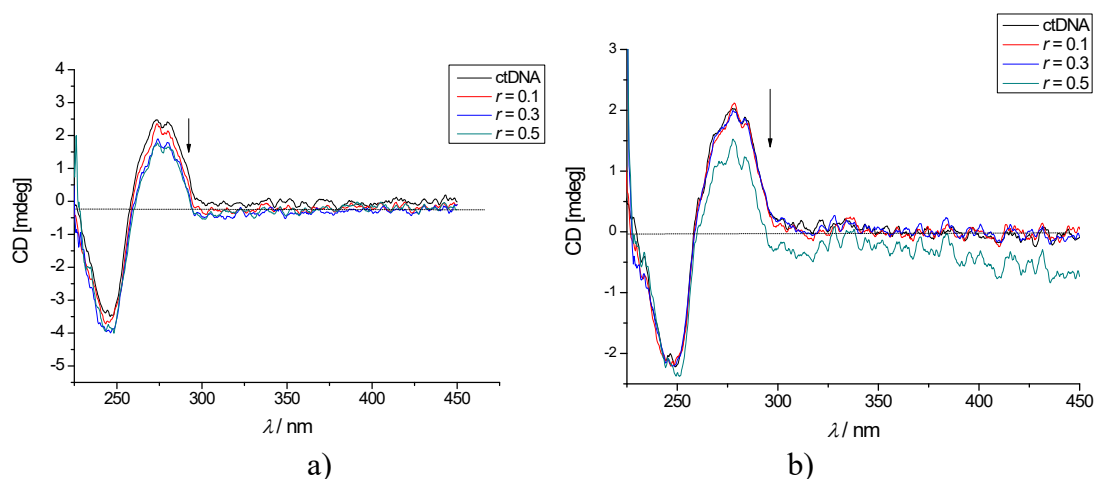


Figure S39. CD titration of ctDNA ($c = 3 \times 10^{-5}$ M) with: a) **2**/ Cu^{2+} ($c = 1 \times 10^{-3}$ M) and b) **3**/ Cu^{2+} ($c = 1 \times 10^{-3}$ M) at different ratio. Done in sodium cacodylate buffer ($\text{pH} = 7.0$, $I = 0.05$ M); $r = [\text{compound}] / [\text{DNA/RNA}]$.

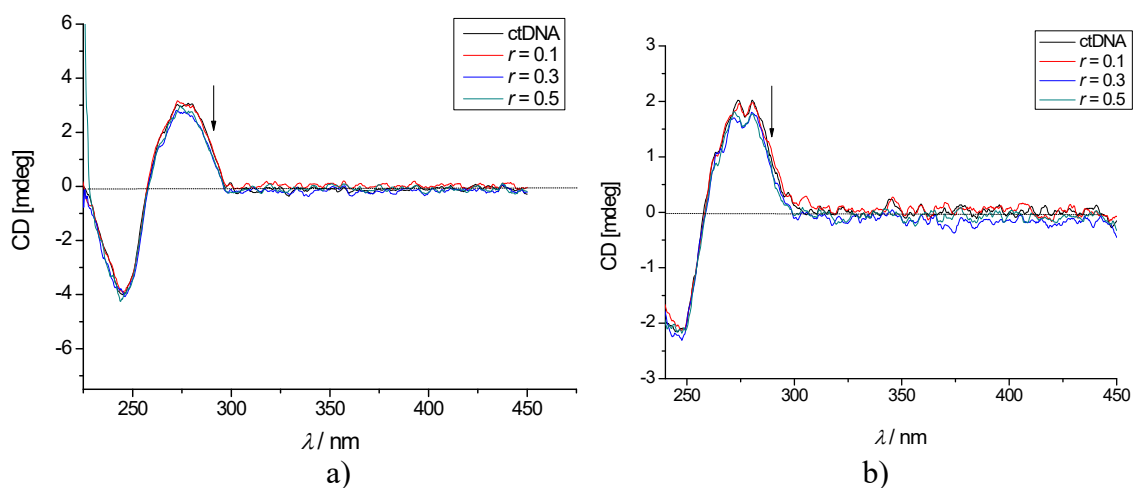


Figure S40. CD titration of ctDNA ($c = 3 \times 10^{-5}$ M) with: a) **2**/ Zn^{2+} ($c = 1 \times 10^{-3}$ M) and b) **3**/ Zn^{2+} ($c = 1 \times 10^{-3}$ M) at different ratio. Done in sodium cacodylate buffer ($\text{pH} = 7.0$, $I = 0.05$ M); $r = [\text{compound}] / [\text{DNA/RNA}]$.

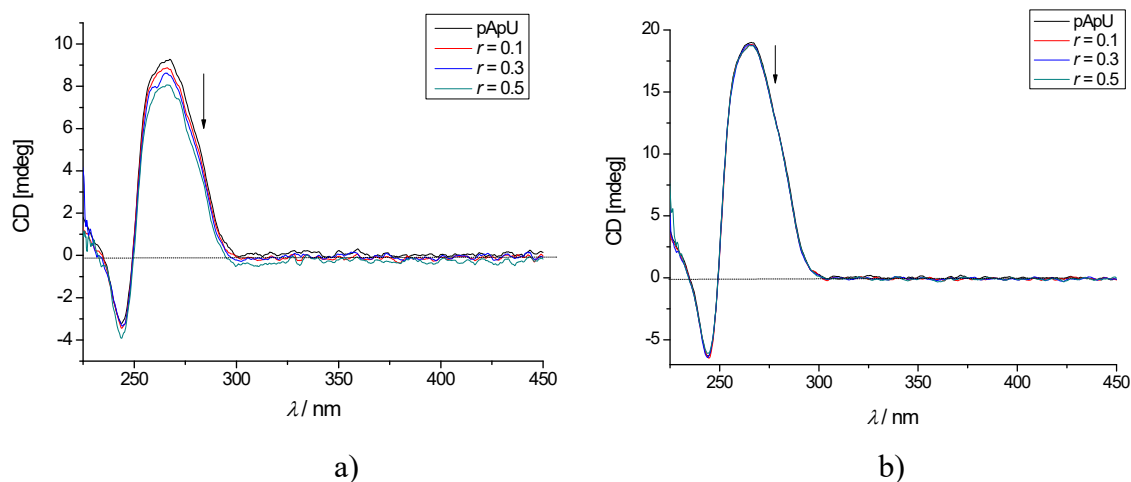


Figure S41. CD titration of pApU ($c = 3 \times 10^{-5}$ M) with: a) **2** ($c = 5 \times 10^{-3}$ M) and b) **3** ($c = 5 \times 10^{-3}$ M) at different ratio. Done in sodium cacodylate buffer (pH = 7.0, $I = 0.05$ M); $r = [\text{compound}] / [\text{DNA/RNA}]$.

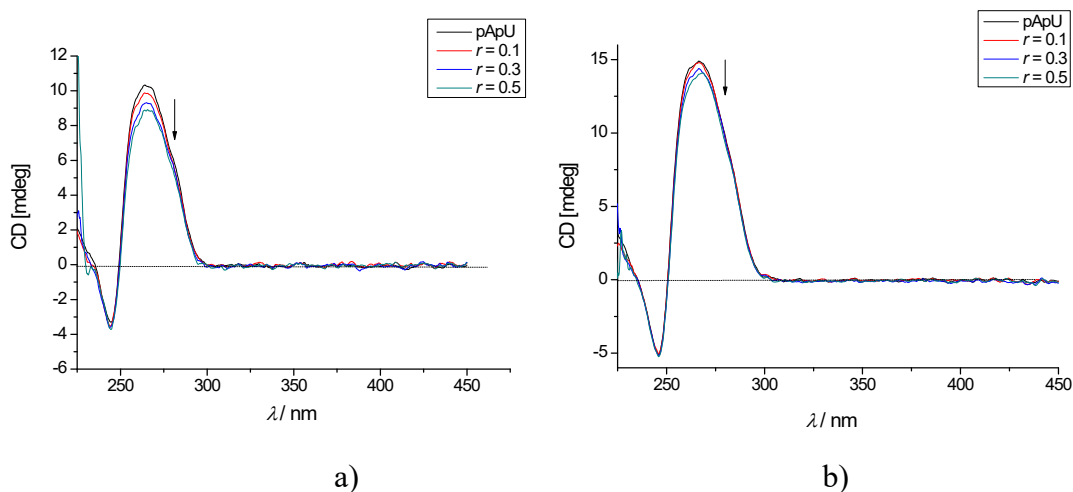


Figure S42. CD titration of pApU ($c = 3 \times 10^{-5}$ M) with: a) **2**/ Cu^{2+} ($c = 5 \times 10^{-3}$ M) and b) **3**/ Cu^{2+} ($c = 5 \times 10^{-3}$ M) at different ratio. Done in sodium cacodylate buffer (pH = 7.0, $I = 0.05$ M); $r = [\text{compound}] / [\text{DNA/RNA}]$.

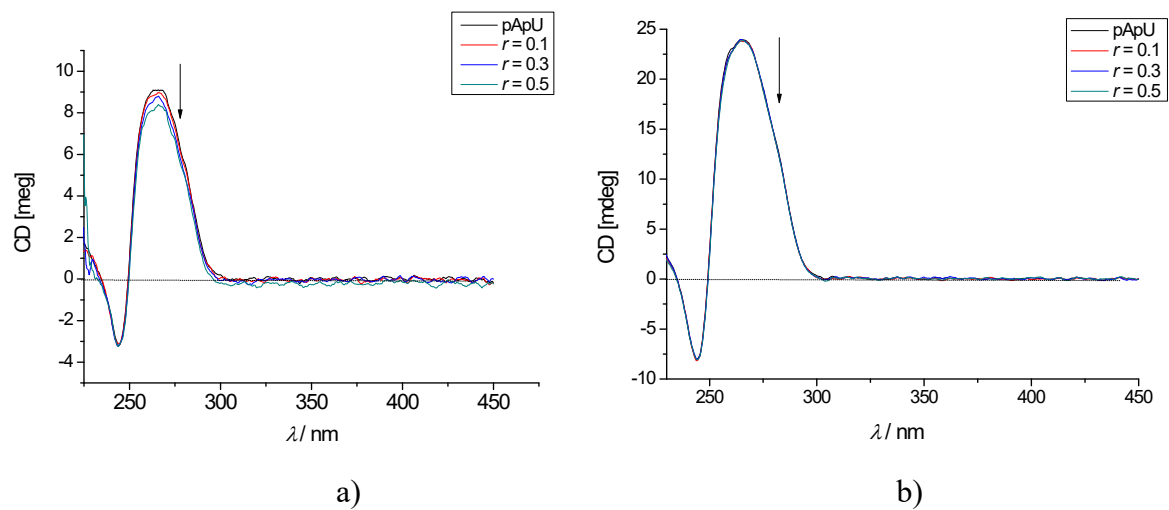


Figure S43. CD titration of pApU ($c = 3 \times 10^{-5}$ M) with: a) **2**/ Zn^{2+} ($c = 5 \times 10^{-3}$ M) and b) **3**/ Zn^{2+} ($c = 5 \times 10^{-3}$ M) at different ratio. Done in sodium cacodylate buffer (pH = 7.0, $I = 0.05$ M); $r = [\text{compound}] / [\text{DNA/RNA}]$.

3.3. Thermal denaturation experiments

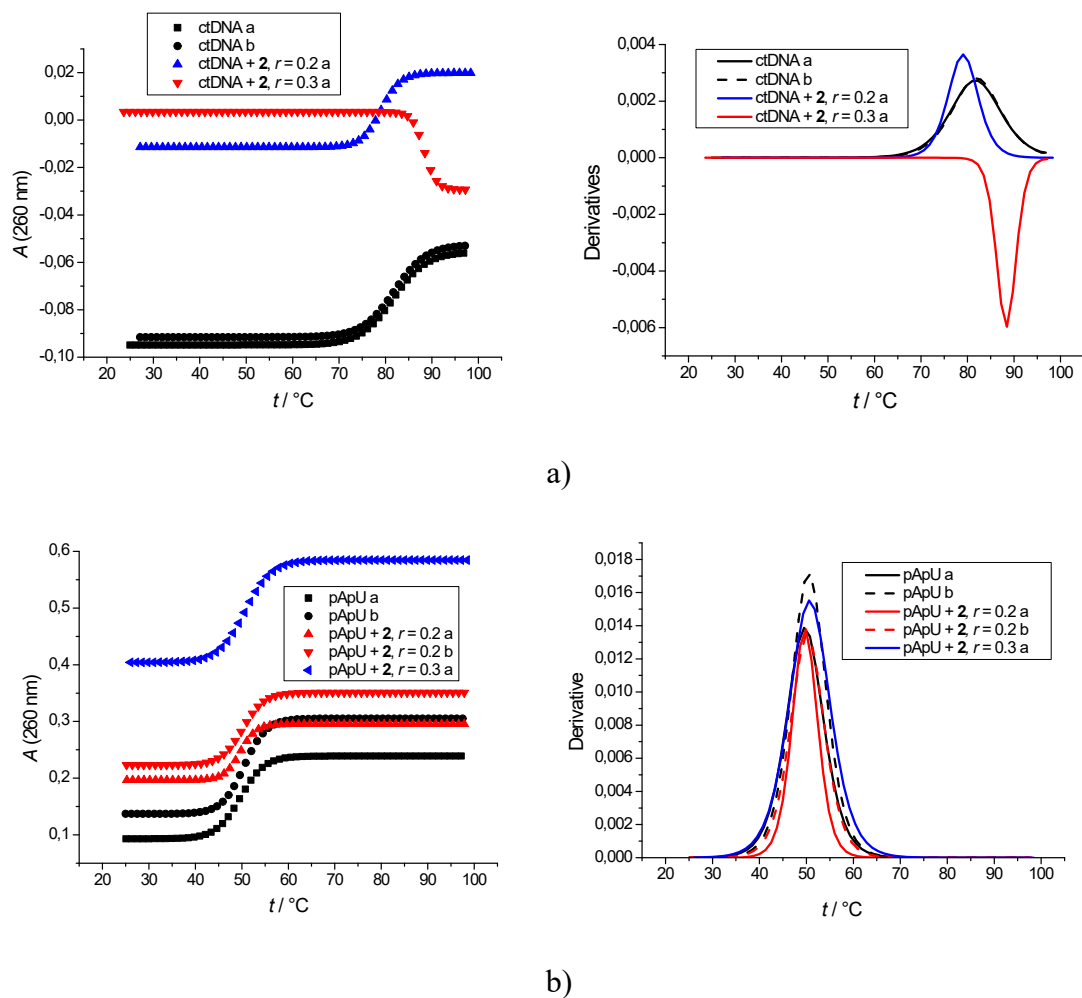
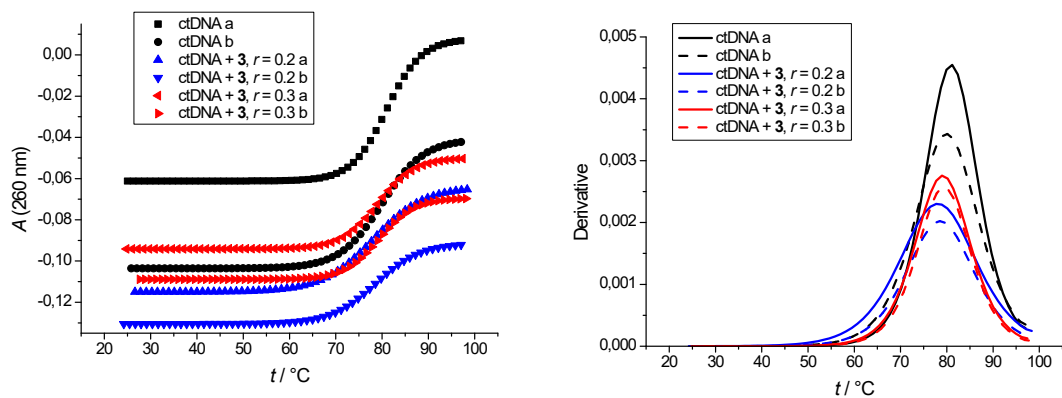
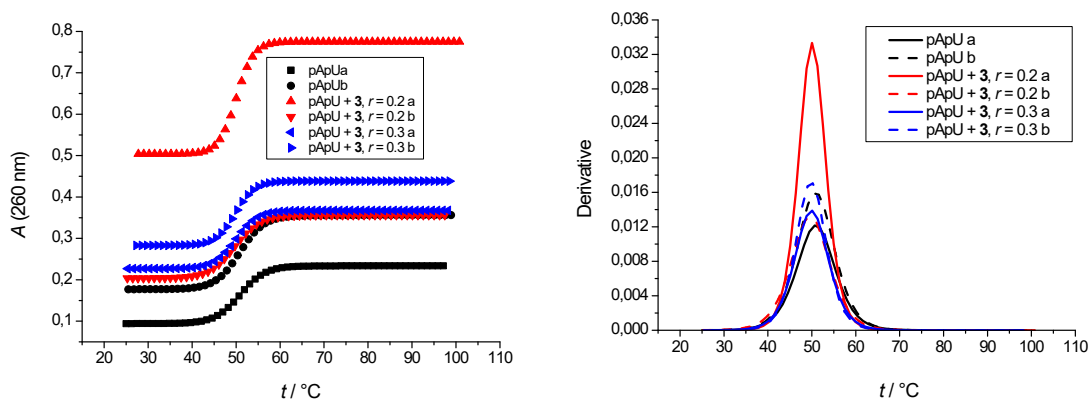


Figure S44. Thermal denaturation curves (left) and derivatives (right) of: a) ctDNA ($c(\text{ctDNA}) = 2.27 \times 10^{-5}\text{ M}$) and b) pApU ($c(\text{pApU}) = 2.27 \times 10^{-5}\text{ M}$) with 2 ($c(2) = 5 \times 10^{-3}\text{ M}$). Done in sodium cacodylate buffer ($\text{pH}=7.0$, $I = 0.05\text{ M}$); $r = [\text{compound}] / [\text{DNA/RNA}]$.



a)



b)

Figure S45. Thermal denaturation curves (left) and derivatives (right) of: a) ctDNA ($c(\text{ctDNA}) = 2.27 \times 10^{-5} \text{ M}$) and b) pApU ($c(\text{pApU}) = 2.27 \times 10^{-5} \text{ M}$) with **3** ($c(\mathbf{3}) = 5 \times 10^{-3} \text{ M}$). Done in sodium cacodylate buffer (pH=7.0, $I = 0.05 \text{ M}$); $r = [\text{compound}] / [\text{DNA/RNA}]$.

Table S3. ΔT_m values for ctDNA and pApU with **2** and **3** at different ratios. Done in sodium cacodylate buffer (pH=7.0, $I = 0.05 \text{ M}$); $r = [\text{compound}] / [\text{DNA/RNA}]$.

		ctDNA	pApU
2	$r = 0.2$	-2	0
	$r = 0.3$	-	+1
3	$r = 0.2$	-2	-1
	$r = 0.3$	-1	-1

$$\Delta T_m = T_{m \text{ poly+compound}} - T_{m \text{ poly}}$$